LA-UR-18-31762
Approved for public release; distribution is unlimited.

Title: Design, analysis and numerical experiments for the virtual element p and hp approximations of elliptic eigenvalue problems

Author(s): Certik, Ondrej
Gardini, Francesca
Manzini, Gianmarco
Mascotto, Lorenzo
Vacca, Giuseppe

Intended for: Report

Issued: 2018-12-18

Design, analysis and numerical experiments for the virtual element p and hp approximations of elliptic eigenvalue problems

O. Čertík [a] , F. Gardini [b] , G. Manzini [c] , L. Mascotto [d] , and G. Vacca [e]

[a] *Group CCS-2, Computer, Computational and Statistical Division, Los Alamos National Laboratory, USA* e-mail: certik@lanl.gov

[b] *Dipartimento di Matematica F. Casorati, Universitá di Pavia, Pavia, Italy* e-mail: francesca.gardini@unipv.it

[c] *Group T-5, Theoretical Division, Los Alamos National Laboratory, USA;* e-mail: gmanzini@lanl.gov

[d] *Fakultät für Mathematik, Universität Wien, Vienna, Austria* e-mail: lorenzo.mascotto@univie.ac.at

[e] *Dipartimento di Matematica e Applicazioni, Universitá degli Studi di Milano Bicocca, Milano, Italy* e-mail: giuseppe.vacca@unimib.it

Abstract

We discuss the p- and the hp-versions of the virtual element method for the approximation of the eigenvalues of elliptic operators with a potential term on polygonal meshes. An application of this model is provided by the Schrödinger equation with a pseudo-potential term. We present in details the analysis of the p-version of the method, proving the exponential convergence in the case of analytic eigenfunctions. The theoretical results are supplied with a wide set of experiments. We also show numerically that, in the case of eigenfunctions with finite Sobolev regularity, an exponential approximation of the eigenvalues in terms of the cubic root of the number of degrees of freedom can be obtained by employing hp-refinements. Importantly, the geometric flexibility of polygonal meshes is exploited in the construction of the hp-spaces.

Key words: virtual element methods, polygonal meshes, eigenvalues, p- and hp-Galerkin methods

1. Introduction

In the last five years, the virtual element method (VEM) [22], has established itself as one of the most ductile and flexible Galerkin methods for the approximation of solutions to partial differential equations (PDEs) on polygonal and polyhedral meshes, i.e., meshes with arbitrarily-shaped polygonal/polyhedral (polytopal, for short) elements. The development of numerical methods for partial differential equations (PDEs) on such kind of meshes has been, indeed, one of the major research themes of the last two decades in the field of numerical analysis. A nonexhaustive list of such methods include the Mimetic Finite Difference method [4, 9, 25, 26, 30, 44, 46, 83, 85–89], the Polygonal Finite Element Method [90, 100, 101], the polygonal Discontinuous Galerkin Finite Element Methods [5, 7, 8, 10, 13–15, 21, 47, 50, 51, 53, 69], the Hybridizable Discontinuous Galerkin and Hybrid High-Order Methods [62–64, 70], the Gradient Discretization method [68, 72, 73], the Finite Volume Method [71], and the BEM-based FEM [97].

The VEM is a generalization of the finite element method (FEM) to polygonal grids, and is based on tools stemming from mimetic finite differences [26, 88]. The main idea of the method is that, to standard piecewise polynomials, additional functions allowing the construction of suitable global spaces are added. Such functions are defined implicitly as solutions to local PDEs and therefore are unknown in closed form. As

a consequence, the exact forms appearing in the weak formulation of the target problem are not computable; rather, they are replaced by suitable discrete counterparts that have to be computable by means of the degrees of freedom and that are based on two main ingredients: projectors into polynomial spaces, and bilinear forms stabilizing the method on the kernel of such projectors.

The VEM, originally proposed for the numerical treatment of second-order elliptic problems [22, 56, 57], was readily extended to linear and nonlinear elasticity [23, 27, 75], plate bending problems [48], Cahn-Hilliard equation [3], Stokes equations [2], Laplace-Beltrami equation [74], Darcy-Brinkam equation [102], discrete topology optimization problems [6], fracture networks problems [39]. The mixed virtual element formulation was proposed in [24, 45]. The nonconforming formulations was proposed for second-order elliptic problems in [16], and later extended to general advection-reaction-diffusion problems, Stokes equation and the biharmonic problems, cf. [11, 40, 55, 58, 104]. A posteriori error estimates can be found in [29, 54]. Last but not least, it is also worth mentioning that the peculiar feature of VEM is the possibility of designing approximation spaces characterized by high continuity properties, cf. [28] and the works on high-order partial differential equations as the biharmonic equations mentioned above..

The aim of the present work is to discuss the approximation of the eigenvalues of certain elliptic operators by means of the VEM. Despite the novelty of this method, virtual elements for the approximation of eigenvalues have been applied to a plethora of different problems, such as the Poisson problem [76, 77], the Poisson problem with a potential term [60], the Steklov eigenvalue problem [92, 93], transmission problems [95], the vibration problem of Kirchhoff plates [94], and the acoustic vibration problem [38]. We highlight that the approximation of eigenvalues with polygonal methods has been targeted in the context of the hybrid-high order method [49] and mimetic finite differences [52].

One of the novelty of the present paper is that we investigate the eigenvalue approximation by means of the VEM employing both the p- and the hp-versions of the method. In the former approach, the convergence is obtained by keeping fixed the mesh and by increasing the dimension of the local spaces. Instead, the latter approach makes use of a combination of the h- and of the p-versions of the FEM, see [17, 99]. In particular, the hp-gospel states that the meshes have to be refined on those elements where the solution to the target problem has a finite Sobolev regularity, whereas the polynomial degree increases in a nonuniform fashion on those elements where the solution is smooth.

The advantage of using the p- and the hp-versions of a Galerkin method over their h-counterpart, is that, in the latter case, the method converges algebraically in terms of the mesh size, with rate depending on the polynomial degree and on the regularity of the solution. On the contrary, exponential convergence can be proven in the former cases; more precisely, for analytic solutions, the p-version converges exponentially in terms of the polynomial degree p, whereas, for solutions with finite Sobolev regularity, the hp-version gives exponential convergence in terms of the cubic root of the number of degrees of freedom. The literature of p- and hp-continuous and discontinuous FEM for the approximation of the eigenvalues is particularly wide. We limit ourselves here to cite the works of Giani and collaborators, see for instance [78–80] and a paper of Sauter [98], where error estimates are proven with bounds that are explicit in the mesh size, in the polynomial degree, and in the eigenvalues; the work [67] focuses instead on hp-adaptive FEM in the framework of eigenvalues in quantum mechanics.

The p- and the hp-versions of VEM have been investigated in a series of work: the analysis for quasi-uniform and geometrically graded meshes was the topic of [33, 34], a p-multigrid algorithm was investigated in [12]; finally, [37] was devoted to hp-residual-based a posteriori error analysis. In all these works, the target problem was the Poisson problem. Therefore, an additional novelty of this paper is that we extend the p- and hp-VEM formulations to the case of more general elliptic problems, namely, we allow for variable diffusivity tensor and for the presence of a (smooth) potential term. With respect to the Poisson case, we face here additional hindrances, partially due to the fact that we employ some special virtual element spaces, that is, the so-called enhanced virtual element spaces [1]: (i) p-best interpolation estimates in enhanced virtual element spaces can be suboptimal; (ii) a stabilization for the L^2 inner product with explicit bounds in terms of p has to be figured out. Moreover, at the practical level, one has to be careful in defining a "clever" basis of the space, since a bad choice could lead to a very ill-conditioned method; in order to avoid such situation, we will resort to the special bases discussed in [65, 91].

As already underlined, we focus on the approximation of the eigenvalues of elliptic operators consisting

of a second order term (with variable diffusion tensor) plus a zero-th order pseudo-potential term. This corresponds to the case of a Schrödinger equation with a pseudo-potential term, which is a basic brick to face more complex problems stemming from the density functional theory [20, 82, 103].

We highlight that the analysis for more general elliptic problems, e.g. including a convections terms, follows combining the techniques of the present paper with those in [32].

The paper is organized as follows. Having introduced the method (including the local and global discrete spaces, and the discrete bilinear forms) and its approximation properties in Section 2, we discuss the convergence analysis in Section 3; here, we use the tools stemming from the Babuška-Osborn theory [18], see also [41].

Section 4 is committed to present a number of numerical experiments including the *p*- and the *hp*-versions of the method; in the latter case, we employ meshes that geometrically graded towards the singularities of the eigenfunctions; the construction of such graded meshes exploits the geometric flexibility of polygonal meshes. The conclusions are stated in Section 5.

Notation. Throughout the paper, we shall employ the standard notation for Sobolev spaces. In particular, given $D \subseteq R^n$, $n = 1, 2$, we denote by $H^s(D)$, $s \in \mathbb{R}_+$, the Sobolev space of order s over Ω and we denote by

$$(\cdot,\cdot)_{s,D}, \qquad |\cdot|_{s,D}, \qquad \|\cdot\|_{s,D},$$

the associated H^s inner product, seminorm, and norm, respectively.

The space $H^{\frac{1}{2}}(\partial D)$, where ∂D is a Lipschitz boundary, is defined as the space of $H^0(\partial D) = L^2(\partial D)$ functions over ∂K, with finite Aronszajn-Slobodeckij seminorm

$$|u|^2_{\frac{1}{2},\partial K} = \int_{\partial D}\int_{\partial D} \frac{|u(\xi)-u(\eta)|^2}{|\xi-\eta|^2} d\xi\, d\eta.$$

The space $H^{-\frac{1}{2}}(\partial D)$ represents the dual space of $H^{\frac{1}{2}}(\partial D)$. Besides, we denote by $\mathbb{P}_\ell(D)$, $\ell \in \mathbb{N}$, the space of polynomials of degree smaller than or equal to ℓ over D, and by π_ℓ its dimension. Instead, given ℓ_1 and ℓ_2 such that $\ell_1 < \ell_2$, the space $\mathbb{P}_{\ell_2}(D) \setminus \mathbb{P}_{\ell_1}(D)$ represents the space of the polynomials of degree ℓ_2, that are orthogonal to the space $\mathbb{P}_{\ell_1}(D)$. Finally, given two positive quantities a and b, we write $a \lesssim b$ in lieu of "there exists a constant c, independent of the mesh size and of the polynomial degree, such that $a \le c\, b$". Moreover, we write $a \approx b$ meaning $a \lesssim b$ and $b \lesssim a$ at the same time.

The continuous problem. Let $\mathbb{K} : \Omega \to \mathbb{R}^{2\times 2}$ be a symmetric positive definite tensor with

$$\mathfrak{k}_*|\mathbf{v}|_{\ell^2} \le (\mathbb{K}\mathbf{v})\cdot\mathbf{v} \le \mathfrak{k}^*|\mathbf{v}|_{\ell^2} \quad \forall \mathbf{v} \in \mathbb{R}^2, \tag{1}$$

where $|\cdot|_{\ell^2}$ denotes the Euclidean norm in $\mathbb{R}^2$, for some given constants $0 < \mathfrak{k}_* \le \mathfrak{k}^*$, and let $V : \Omega \to \mathbb{R}$ be such that

$$0 \le \nu_* \le V \le \nu^*, \tag{2}$$

for some given constants ν_* and ν^*.

Given a domain $\Omega \subset \mathbb{R}^2$, we look for a function u and for a positive real number λ satisfying

$$\begin{cases} -\mathrm{div}(\mathbb{K}\cdot\nabla u) + V\, u = \lambda u & \text{in } \Omega \\ u = 0 & \text{on } \partial\Omega. \end{cases} \tag{3}$$

Note that u is defined up to a multiplicative factor. We fix $\|u\|_{0,\Omega} = 1$.

In weak formulation, the eigenvalue problem (3) reads

$$\begin{cases} \text{find } (\lambda, u) \in \mathbb{R}\times H^1_0(\Omega) \text{ with } \|u\|_{0,\Omega} = 1 \text{ such that} \\ a(u,v) + b(u,v) = \lambda c(u,v) \quad \forall v \in H^1_0(\Omega), \end{cases} \tag{4}$$

where we have set

$$a(u,v) = (\mathbb{K}\nabla u, \nabla v)_{0,\Omega}, \quad b(u,v) = (Vu, v)_{0,\Omega}, \quad c(u,v) = (u,v)_{0,\Omega} \quad \forall u,\, v \in H^1(\Omega). \tag{5}$$

We will also make use of the source problem associated with (4). Given $f \in H^1(\Omega)$,

$$\begin{cases} \text{find } u \in H^1_0(\Omega) \text{ such that} \\ a(u,v) + b(u,v) = c(f,v) \quad \forall v \in H^1_0(\Omega). \end{cases} \tag{6}$$

We define the solution operator $T \in \mathcal{L}(H^1(\Omega))$ of the source problem (6) as

$$\mathcal{B}(Tf, v) = c(f,v) \quad \forall v \in H^1_0(\Omega),$$

where we have set $\mathcal{B}(\cdot,\cdot) = a(\cdot,\cdot) + b(\cdot,\cdot)$. The operator T is self-adjoint, compact (thanks to the Sobolev embedding theorems), and positive definite.

We observe that, given $(\lambda, w) \in \mathbb{R} \times H^1_0(\Omega)$ an eigenmode solution to (4), then

$$a(w,v) + b(w,v) = c(\lambda w, v) = a(T\lambda w, v) + b(T\lambda w, v) \quad \forall w \in H^1_0(\Omega).$$

Thus, $T(\lambda w) = w$ and then $T(w) = \frac{1}{\lambda} w$, which means that $(\frac{1}{\lambda}, w)$ is an eigenmode of T. As a consequence, in order to approximate the eigenfunctions and the eigenvalues of the problem (4), it suffices to approximate the eigenfunctions and eigenvalues of T. The issue of approximating the eigenfunctions and eigenvalues of T will be tackled with the tools provided by the Babŭska-Osborn theory [18].

2. The virtual element method

In this section, we discuss the virtual element method tailored for the approximation of the solutions to problem (4), and we discuss h- and p-approximation properties of the functions in such spaces.

More precisely, after having introduced the concept of regular polygonal decompositions in Section 2.1, in Section 2.2 we construct the virtual element spaces and we describe their h- and p-approximation properties; the definition of the discrete bilinear forms is instead the topic of Section 2.3, where a particular emphasis is put on the analysis of the stabilizations with explicit bounds in terms of the mesh size h and the "polynomial" degree p. Finally, Section 2.4 is devoted to state the method.

2.1. *Polygonal meshes*

Given $\Omega \subset \mathbb{R}^2$, we introduce here the concept of regular polygonal decompositions and some useful notation, instrumental for the description of the method.

Let $\{\mathcal{T}_n\}_{n\in\mathbb{N}}$ be a sequence of conforming polygonal decompositions of Ω, i.e., for all $n \in \mathbb{N}$, $\mathcal{T}_n$ is a collection of polygons, such that the intersection of two different polygons is either the empty set, a vertex, or a collection of edges.

We set for future convenience $\mathcal{E}_n$, $\mathcal{E}_n^B$, and $\mathcal{E}_n^I$ the set of edges, of boundary edges, and internal edges of $\mathcal{T}_n$, respectively; moreover, we set $\mathcal{E}^K$ the set of edges of K and n^K its cardinality. The diameter of the elements $K \in \mathcal{T}_n$, the mesh size of $\mathcal{T}_n$, and the length of the edges $e \in \mathcal{E}_n$, are denoted by

$$h_K = \operatorname{diam}(K), \quad h = \max_{K\in\mathcal{T}_n} h_K, \quad h_e = \operatorname{length}(e),$$

respectively.

In the forthcoming analysis, we will make use of the two following assumptions. For all $n \in \mathbb{N}$, there exists a positive constant γ independent of the discretization parameters such that

(D1) for all $K \in \mathcal{T}_n$ and for all $e \in \mathcal{E}^K$, it holds that h_e is larger than or equal to γh_K;

(D2) every $K \in \mathcal{T}_n$ is star-shaped with respect to at least one ball, with radius larger than or equal to γh_K.

We underline that the assumptions (**D1**) and (**D2**) could be in principle weakened, yet retaining analogous approximation properties of the method, as discussed in [36, 43, 59].

Given $\mathcal{T}_n$ a polygonal decomposition of Ω, we define the broken Sobolev seminorm

$$|\cdot|^2_{1,\mathcal{T}_n} = \sum_{K\in\mathcal{T}_n} |\cdot|^2_{1,K}. \tag{7}$$

Moreover, we introduce a triple of operators

$$\Pi_\ell^{0,\widetilde{\Omega}} : L^2(\widetilde{\Omega}) \to \mathbb{P}_\ell(\widetilde{\Omega}), \quad (\Pi_\ell^{0,\widetilde{\Omega}} u - u, q_\ell)_{0,\widetilde{\Omega}} = 0 \quad \forall u \in L^2(\Omega),\ \forall q_\ell \in \mathbb{P}_\ell(\widetilde{\Omega}), \tag{8}$$

$$\Pi_\ell^{\nabla,\widetilde{\Omega}} : H^1(\widetilde{\Omega}) \to \mathbb{P}_\ell(\widetilde{\Omega}), \quad \begin{cases} (\nabla\Pi_\ell^{\nabla,\widetilde{\Omega}} u - \nabla u, \nabla q_\ell)_{0,\widetilde{\Omega}} = 0 \\ \displaystyle\int_{\partial K} v_n - \Pi_\ell^{\nabla,\widetilde{\Omega}} v_n = 0, \end{cases} \quad \forall u \in H^1(\Omega),\ \forall q_\ell \in \mathbb{P}_\ell(\widetilde{\Omega}), \tag{9}$$

for some measurable set $\widetilde{\Omega} \subseteq \mathbb{R}^2$ and for some $\ell \in \mathbb{N}$. In the following, we will denote by $\Pi_\ell^{0,\widetilde{\Omega}}$ also the vector version of the L^2 projector defined in (8).

We also consider the following simplifying assumption:
(A) the coefficients $\mathbb{K}$ and V in (3) are piecewise analytic over $\mathcal{T}_n$, for all $n \in \mathbb{N}$.

2.2. *Virtual element spaces*

In the present section, we introduce the local and global virtual element spaces for the problem (4) and we study their h- and p-approximation properties.

Given an element $K \in \mathcal{T}_n$ and the "polynomial" degree p, we define the auxiliary space

$$\widetilde{V_n}(K) = \{v_n \in \mathcal{C}^0(\overline{K}) \mid \Delta v_n \in \mathbb{P}_{p-1}(K),\ v_{n|e} \in \mathbb{P}_p(e)\, \forall e \in \mathcal{E}^K\}.$$

The local virtual element space over the element K reads

$$V_n(K) = \left\{ v_n \in \widetilde{V_n}(K) \mid \int_K (v_n - \Pi_p^{\nabla,K} v_n) m_\alpha = 0 \quad \forall m_\alpha \in \mathbb{P}_{p-1}(K) \setminus \mathbb{P}_{p-2}(K) \right\}. \tag{10}$$

The local space $V_n(K)$ has been constructed in the spirit of the enhanced virtual element space, see [1]. It is essential to underline that the local virtual element space $V_n(K)$ contains the space of polynomials of degree smaller than or equal to p.

We recall from [31], that $V_n(K)$can be endowed with the following set of unisolvent degrees of freedom. Given $v_n \in V_n(K)$, for all $K \in \mathcal{T}_n$,

- for all the vertices $\{\nu_i\}_{i=1}^{n^K}$ of K, the point-values $v_n(\nu_i)$, for all $i = 1, \dots, n^K$;
- for all edges $e \in \mathcal{E}^K$, the point-values at $p-1$ distinct internal points of e (e.g. at the $p-1$ internal Gauß-Lobatto nodes);
- given $\{m_\alpha\}_{\alpha=1}^{\pi_{p-2}}$, where we recall that π_{p-2} denotes the dimension of $\mathbb{P}_{p-2}(K)$, *any* basis of $\mathbb{P}_{p-2}(K)$ such that m_α is invariant under homothetic transformation for all $\alpha = 1, \dots, \pi_{p-2}$, the scaled moments

$$\frac{1}{|K|} \int_K v_n m_\alpha. \tag{11}$$

In the original VEM approach [31], as well as in the majority of the literature, the basis $\{m_\alpha\}_{\alpha=1}^{\pi_{p-2}}$ is chosen as the basis of (scaled and shifted with the barycenter of the element) monomials. However, in presence of very distorted elements or for a high "polynomial" degree p, this choice may result in a loss of accuracy in the method; alternative choices tackling the high-order case are available in literature [65, 91], and will be pinpointed in Section 4.

Having at disposal the set of local unisolvent degrees of freedom $\{\mathrm{dof}_\ell\}_{j=1}^{\dim(V_n(K))}$, we introduce the canonical basis $\{\mathrm{dof}_\ell\}_{j=1}^{\dim(V_n(K))}$ as $\mathrm{dof}_j(\varphi_\ell) = \delta_{j,\ell}$, where $\delta_{j,\ell}$ denotes the Kronecker delta.

Remark 1 *The reason why we define scaled moments with respect to polynomial basis functions that are invariant under homothetic transformations is that, by doing so, the canonical basis consists of functions with energy invariant under the scaling of the elements.*

Importantly, the functions in local virtual element spaces, as they are solutions to local Poisson problem problems, are known explicitly only at the boundary of the element, but are unknown in closed form at the interior. Therefore, the exact bilinear forms are not computable; rather, they have to be replaced by

proper discrete counterparts avoiding the evaluation of trial and test functions at the integration points, see Section 3.

We also highlight that the choice of the degrees of freedom allows to compute *explicitly* the following quantities, see e.g. [32]:

$$\Pi_{p-1}^{0,K} u_n, \qquad \Pi_p^{\nabla,K} u_n, \qquad \Pi_{p-1}^{0,K}(\nabla u_n) \qquad \forall u_n \in V_n(K),$$

where the projectors $\Pi_{p-1}^{0,K}$ and $\Pi_p^{\nabla,K}$ are defined in (8) and (9), respectively, and where, with a slight abuse of notation, $\Pi_{p-1}^{0,K}(\nabla u_n)$ is the vector counterpart of the L^2 projector in (8). For the sake of clarity, we will henceforth denote the three projectors as Π_{p-1}^0, Π_p^∇, and Π_{p-1}^0, respectively.

The global space is built in an H^1-conforming fashion:

$$V_n = \{v_n \in C^0(\overline{\Omega}) \cap H_0^1(\Omega) \mid v_{n|K} \in V_n(K) \text{ for all } K \in \mathcal{T}_n\}.$$

The set of global degrees of freedom is obtained by a standard coupling of the local ones.

We underline that it is also possible to build nonconforming spaces (à la Crouzeix-Raviart), see e.g. [16, 76]. At any rate, we stick here to the H^1-conforming case.

The remainder of the section is devoted to prove some best approximation results in polynomial and virtual element spaces. We begin by recalling from [33, Lemma 4.2] the following *hp*-best polynomial approximation results over shape regular polygons.

Theorem 1 (*hp*-best polynomial approximation error over polygons) *Given $K \in \mathcal{T}_n$ and $u \in H^{s+1}(K)$, $s \geq 0$, for all $p \in \mathbb{N}$, there exists $u_\pi \in \mathbb{P}_p(K)$ such that*

$$|u - u_\pi|_{\ell,K} \lesssim \frac{h_K^{\min(p,s)+1-\ell}}{p^{s+1-\ell}} \|u\|_{s+1,K} \quad \forall \ell \geq 0, \quad 0 \leq \ell \leq s.$$

Next, we prove an auxiliary result which will be instrumental for proving an *hp*-best interpolation result in enhanced virtual element spaces. To this aim, we first introduce $\widetilde{\mathcal{T}}_n$, a subtriangulation of Ω obtained as follows. For every $K \in \mathcal{T}_n$, we connect its vertices to the center of any ball (with maximal radius) with respect to which K is star-shaped, see the geometric assumption (**D2**). The union of such triangles is denoted by $\widetilde{\mathcal{T}}_n$. Associated with the subtriangulation $\widetilde{\mathcal{T}}_n$, we define the broken Sobolev seminorm $|\cdot|^2_{1,\widetilde{\mathcal{T}}_n}$ as in (7).

Theorem 2 *For every $u \in H^1(\Omega)$, there exists $u_I \in V_n$ such that*

$$|u - u_I|_{1,\Omega} \lesssim p(|u - u_\pi|_{1,\mathcal{T}_n} + |u - \widetilde{u}_\pi|_{1,\widetilde{\mathcal{T}}_n}) \tag{12}$$

for all u_π and $\widetilde{u}_\pi$ piecewise continuous polynomials of degree p over $\mathcal{T}_n$ and $\widetilde{\mathcal{T}}_n$, respectively.

Proof. The proof employs some tools from [33, Lemma 4.3], [34, Theorem 2], and [54, Theorem 11]. We assume without loss of generality that $p \geq 2$ (we are interested only in the asymptotic behavior of p).

Given $u \in H^1(\Omega)$, we start by defining the auxiliary interpolant $v_I \in H^1(\Omega)$ whose restriction on K, for all $K \in \mathcal{T}_n$, belongs to the space $\widetilde{V_n}(K)$, as

$$\begin{cases} -\Delta v_I = -\Delta u_\pi & \text{in } K \\ v_I = \widetilde{u}_\pi & \text{on } \partial K, \end{cases}$$

for some u_π and $\widetilde{u}_\pi$ piecewise continuous polynomials of degree p over $\mathcal{T}_n$ and $\widetilde{\mathcal{T}}_n$, respectively. Following [33, Lemma 4.3] or [92, Proposition 4.2], one shows

$$|u - v_I|_{1,\Omega} \leq |u - \widetilde{u}_\pi|_{1,\widetilde{\mathcal{T}}_n} + 2|u - u_\pi|_{1,\mathcal{T}_n}. \tag{13}$$

Next, we introduce an interpolant u_I in the space V_n, defined on all $K \in \mathcal{T}_n$, as

$$\mathrm{dof}_i(u_I - v_I) = 0 \qquad \forall i = 1, \ldots, \dim(V_n(K)), \quad \forall K \in \mathcal{T}_n \tag{14}$$

where we recall that $\{\mathrm{dof}_i\}_{i=1}^{\dim(V_n(K))}$ is the set of degrees of freedom of $V_n(K)$, for all $K \in \mathcal{T}_n$. It can be proven that (14) implies

$$\Pi_p^\nabla u_I = \Pi_p^\nabla v_I \tag{15}$$

in $K \in \mathcal{T}_n$, for all $K \in \mathcal{T}_n$.

Setting $q_{p-1} := \Delta(u_I - v_I) \in \mathbb{P}_{p-1}(K)$, an integration by parts, together with the definitions of u_I and of v_I and (15), yields

$$\begin{aligned}
|u_I - v_I|^2_{1,K} &\underbrace{=}_{(14)} \int_K -q_{p-1}(u_I - v_I) \underbrace{=}_{(14)} \int_K (I - \Pi^0_{p-2}) q_{p-1} (v_I - u_I) \\
&\underbrace{=}_{(10)} \int_K (I - \Pi^0_{p-2}) q_{p-1} (v_I - \Pi^\nabla_p v_I) = \underbrace{=}_{(15)} \int_K (I - \Pi^0_{p-2}) q_{p-1} (v_I - \Pi^\nabla_p v_I) \\
&= \int_K q_{p-1} (v_I - \Pi^\nabla_p v_I) \leq \|q_{p-1}\|_{0,K} \|(I - \Pi^0_{p-1})(v_n - \Pi^\nabla_p v_n)\|_{0,K} \\
&\lesssim \|q_{p-1}\|_{0,K} h_K (p-2)^{-1} \|v_n - \Pi^\nabla_p v_n\|_{0,K} \leq \|q_{p-1}\|_{0,K} h_K p^{-1} \|v_n - \Pi^\nabla_p v_n\|_{0,K},
\end{aligned} \tag{16}$$

where the last but one inequality follows from the properties of the L^2 projector, the fact that $p \geq 2$, and Theorem 1.

Next, we recall the p-polynomial inverse estimate [34, equation (33)]

$$\|q_{p-1}\|_{0,K} = \|\Delta(u_I - v_I)\|_{0,K} \lesssim \frac{p^2}{h_K} |u_I - v_I|_{1,K}. \tag{17}$$

Combining (16) and (17), we deduce that

$$|u_I - v_I|^2_{1,K} \lesssim p |u_I - v_I|_{1,K} \|v_I - \Pi^\nabla_p v_I\|_{1,K}.$$

This, together with a Poincaré inequality (which applies since $v_I - \Pi^\nabla_p v_I$ has zero average on ∂K) and the properties of the projector Π^∇_p (which is the best approximation in H^1), entails

$$\begin{aligned}
|u_I - v_I|_{1,K} &\lesssim p \|v_I - \Pi^\nabla_p v_I\|_{1,K} \lesssim p |v_I - \Pi^\nabla_p v_I|_{1,K} \leq p |v_I - u_\pi|_{1,K} \\
&\lesssim p \left(|u - v_I|_{1,K} + |u - u_\pi|_{1,K} \right).
\end{aligned} \tag{18}$$

Hence, a triangle inequality, together with (13) and (18), leads to

$$|u - u_I|_{1,K} \leq |u - v_I|_{1,K} + |u_I - v_I|_{1,K} \lesssim p(|u - v_I|_{1,K} + |u - u_\pi|_{1,K}) \lesssim p(|u - \widetilde{u}_\pi|_{1,K} + |u - u_\pi|_{1,K}),$$

which is the claim. □ We have now all the tools so as to prove an hp-best interpolation error result by means of functions in virtual element spaces.

Corollary 3 (hp-best interpolation error in virtual element spaces) *Given $u \in H^1_0(\Omega)$ piecewise in $H^{s+1}(K)$ for all $K \in \mathcal{T}_n$, $s \geq 0$, there exists $u_I \in V_n$ such that*

$$|u - u_I|_{1,\Omega} \lesssim \frac{h^{\min(p,s)}}{p^{s-1}} \left(\sum_{K \in \mathcal{T}_n} \|u\|^2_{s+1,K} \right)^{\frac{1}{2}}.$$

Proof. The assertion follows from Theorem 2, applying [19, Theorem 4.6] and Theorem 1 to the first and second terms term on the right-hand side of (12), respectively. □

We point out that the best interpolation error proven in Corollary 3 is suboptimal of one power of p with respect to its counterpart in standard VE spaces, see [33, Lemma 4.3]. As a consequence, it will turn out that performing a pure p-version of the method on a test case with a finite Sobolev regularity solution could lead to a suboptimal rate of convergence.

However, assuming that the target function u is analytic, the rate of convergence of the p-version of a Galerkin method (such as FEM [99] and VEM [33]) is typically exponential in terms of the polynomial degree p; therefore, the suboptimal polluting factor p can be absorbed in the exponential term; see the forthcoming Theorem 11 for a more precise statement. In case instead one considers a test case with exact solution having finite Sobolev regularity, one may proceed with hp-refinement techniques, which lead however to exponential convergence, this time in terms of the cubic root of the number of degrees of freedom. This procedure will be numerically investigated in the forthcoming Section 4.2.

2.3. *Discrete bilinear forms*

Having recalled that the functions in virtual element spaces are unknown in closed form and therefore, *rebus sic stantibus*, it is not possible to implement the method, the aim of the present section is to define discrete bilinear forms that are computable via the degrees of freedom of the space.

We begin with the discrete counterpart of the bilinear form $a(\cdot,\cdot)$, which is constructed in the spirit of [32]. We first define the local discrete bilinear forms. For all $K \in \mathcal{T}_n$,

$$a_n^K(u_n, v_n) = \sum_{K\in\mathcal{T}_n} (\mathbb{K}\Pi^0_{p-1}\nabla u_n, \Pi^0_{p-1}\nabla v_n) + S_1^K((I-\Pi_p^\nabla)u_n, (I-\Pi_p^\nabla)v_n) \quad \forall u_n,\, v_n \in H^1(K), \tag{19}$$

where $S_1^K : \ker(\Pi_p^\nabla)^2 \to \mathbb{R}$ is any bilinear form computable via the set of local degrees of freedom, satisfying

$$\alpha_*(p)|v_n|^2_{1,K} \le S_1^K(v_n, v_n) \le \alpha^*(p)|v_n|^2_{1,K} \quad \forall v_n \in \ker(\Pi_p^\nabla), \tag{20}$$

for some positive constants $\alpha_*(p)$ and $\alpha^*(p)$ independent of h_K but not of p. We recall that $\Pi^0_{p-1}\nabla u_n$ is explicitly known. The global discrete bilinear form is instead given by

$$a_n(u_n, v_n) = \sum_{K\in\mathcal{T}_n} a_n^K(u_n, v_n).$$

The following result concerns the continuity and the coercivity of a_n^K.

Lemma 4 *For all $K \in \mathcal{T}_n$, the local discrete bilinear form a_n^K in (19) satisfies the following properties:*

$$\min(\mathfrak{k}_*, \alpha_*(p))|v_n|^2_{1,K} \le a_n^K(u_n, v_n) \le (\mathfrak{k}^* + \alpha^*(p))|v_n|^2_{1,K} \quad \forall v_n \in V_n(K), \tag{21}$$

where we recall that $\mathfrak{k}_*$ and $\mathfrak{k}^*$ are introduced in (1), whereas $\alpha_*(p)$ and $\alpha^*(p)$ are defined in (20).

Proof. We begin with the upper bound:

$$\begin{aligned} a_n^K(v_n, v_n) &= (\mathbb{K}\Pi^0_{p-1}\nabla v_n, \Pi^0_{p-1}\nabla v_n)_{0,K} + S_1^K((I-\Pi_p^\nabla)v_n, (I-\Pi_p^\nabla)v_n) \\ &\le \mathfrak{k}^*\|\Pi^0_{p-1}\nabla v_n\|^2_{0,K} + \alpha^*(p)|(I-\Pi_p^\nabla)v_n|^2_{1,K} \le \mathfrak{k}^*\|\nabla v_n\|^2_{0,K} + \alpha^*(p)\|\nabla v_n\|^2_{0,K} \\ &\le (\mathfrak{k}^* + \alpha^*(p))|v_n|^2_{1,K}. \end{aligned}$$

For what concerns the lower bound, we have

$$\begin{aligned} a_n^K(v_n, v_n) &= (\mathbb{K}\Pi^0_{p-1}\nabla v_n, \Pi^0_{p-1}\nabla v_n)_{0,K} + S_1^K((I-\Pi_p^\nabla)v_n, (I-\Pi_p^\nabla)v_n) \\ &\ge \mathfrak{k}_*\|\Pi^0_{p-1}\nabla v_n\|^2_{0,K} + \alpha_*(p)|(I-\Pi_p^\nabla)v_n|^2_{1,K} \\ &\ge \mathfrak{k}_*\|\Pi^0_{p-1}\nabla v_n\|^2_{0,K} + \alpha_*(p)\|(I-\Pi^0_{p-1})\nabla v_n\|^2_{0,K} \\ &\ge \min(\mathfrak{k}_*, \alpha_*(p))|v_n|^2_{1,K}. \end{aligned}$$

□

For what concerns the discrete counterpart of $b(\cdot,\cdot)$, we pick

$$b_n(u_n, v_n) = \sum_{K\in\mathcal{T}_n} b_n^K(u_n, v_n) = \sum_{K\in\mathcal{T}_n} (V\Pi^0_{p-1}u_n, \Pi^0_{p-1}v_n)_{0,K} \quad \forall u_n,\, v_n \in H^1(K), \tag{22}$$

which is computable, owing to the fact that Π^0_{p-1} is available in closed form, from the degrees of freedom; we are here assuming to be able to compute exactly integrals of given smooth functions (otherwise, a sufficiently good quadrature formula is enough).

Finally, we focus on the discrete counterpart of $c(\cdot,\cdot)$:

$$\begin{aligned} c_n(u_n, v_n) &= \sum_{K\in\mathcal{T}_n} c_n^K(u_n, v_n) \\ &= \sum_{K\in\mathcal{T}_n} (\Pi^0_{p-1}u_n, \Pi^0_{p-1}v_n)_{0,K} + S_0^K((I-\Pi^0_{p-1})u_n, (I-\Pi^0_{p-1})v_n) \quad \forall u_n,\, v_n \in H^1(K), \end{aligned} \tag{23}$$

where $S_0^K : \ker(\Pi^0_{p-1})^2 \to \mathbb{R}$ is a bilinear form computable via the set of the local degrees of freedom, such that

$$S_0^K(v_n, v_n) \ge \beta_*(p)\|v_n\|^2_{0,K} \quad \forall v_n \in \ker(\Pi^0_{p-1}), \tag{24}$$

and such that

$$S_0^K(v_n - \Pi_{p-1}^0 v_n, v_n - \Pi_{p-1}^0 v_n) \leq h_K^2 \beta^* |v_n - \Pi_{p-1}^\nabla v_n|_{1,K}^2 \quad \forall v_n \in V_n(K), \tag{25}$$

for some positive constants $\beta_*(p)$ independent of h_K but not of p, and β^* independent of h_K and p.

The following result concerns the continuity and the coercivity of c_n.

Lemma 5 *The discrete bilinear form c_n in (23) satisfies the two following properties:*

$$\min(1, \beta_*(p)) \|v_n\|_{0,K}^2 \leq c_n^K(u_n, v_n) \leq \max(1, \beta^*)(\|u_n\|_{0,K}^2 + h_K^2 |v_n|_{1,K}^2) \quad \forall v_n \in V_n(K), \tag{26}$$

where we recall that $\beta_*(p)$ and β^* are introduced in (24) and (25), respectively.

Proof. The proof of the lower bound is the same as that of its counterpart in Lemma 4. For what concerns the upper bound, we proceed as follows:

$$\begin{aligned} c_n^K(v_n, v_n) &= (\Pi_{p-1}^0 v_n, \Pi_{p-1}^0 v_n)_{0,K} + S_0^K((I - \Pi_{p-1}^0)v_n, (I - \Pi_{p-1}^0)v_n) \\ &\leq \|v_n\|_{0,K}^2 + h_K^2 \beta^* |v_n - \Pi_{p-1}^\nabla v_n|_{1,K}^2 \leq \|v_n\|_{0,K}^2 + h_K^2 \beta^* |v_n|_{1,K}^2 \\ &\leq \max(1, \beta^*)(\|v_n\|_{0,K}^2 + h_K^2 |v_n|_{1,K}^2). \end{aligned}$$

□

Remark 2 *Following [77], one could in principle construct a method by removing the stabilization S_0^K. The reason for which we stabilize the bilinear form c_n is simply that otherwise the resulting matrix could be singular.*

2.3.1. *Explicit choices for the stabilizations S_0^K and S_1^K*

In this section, we introduce two *explicit* stabilizing bilinear forms S_1^K and S_0^K, see (20) and (24), respectively, with explicit continuity and coercivity bounds in terms of p on $\alpha_*(p)$, $\alpha^*(p)$, and $\beta_*(p)$.

Theorem 6 *Given*

$$S_1^K(u_n, v_n) = \frac{p^2}{h_K^2}(\Pi_{p-2}^0 v_n, \Pi_{p-2}^0 v_n)_{0,K} + \frac{p}{h_K}(u_n, v_n)_{0,\partial K} \quad \forall u_n,\, v_n \in \ker(\Pi_p^\nabla),\, \forall K \in \mathcal{T}_n, \tag{27}$$

the following bounds on the constants $\alpha_*(p)$ and $\alpha^*(p)$ in (20) hold true:

$$\alpha_*(p) \gtrsim p^{-5}, \quad \alpha^*(p) \lesssim p^2. \tag{28}$$

Proof. The proof is analogous to that of [34, Theorem 2]. Notwithstanding, we show a few details, since here we employ enhanced virtual element spaces, which are slightly different from the standard ones in [34].

More precisely, we only show some details regarding the bound on $\alpha_*(p)$. Given $K \in \mathcal{T}_n$ and $v_n \in \ker(\Pi_p^\nabla)$, it holds true that

$$|v_n|_{1,K}^2 = \int_K \nabla v_n \cdot \nabla v_n = \int_K -\Delta v_n\, v_n + \int_{\partial K} \partial_{\mathbf{n}} v_n\, v_n = \int_K -\Delta v_n\, \Pi_{p-1}^0 v_n + \int_{\partial K} \partial_{\mathbf{n}} v_n\, v_n.$$

Using the enhancing constraints in (10) and the fact that v_n belongs to $\ker(\Pi_p^\nabla)$, we deduce

$$\begin{aligned} |v_n|_{1,K}^2 &= \int_K -\Delta v_n\, \Pi_{p-2}^0 v_n + \int_{\partial K} \partial_{\mathbf{n}} v_n\, v_n \\ &\leq \|\Delta v_n\|_{0,K} \|\Pi_{p-2}^0 v_n\|_{0,K} + \|\partial_{\mathbf{n}} v_n\|_{-\frac{1}{2},\partial K} \|v_n\|_{\frac{1}{2},\partial K}. \end{aligned}$$

Having this, it suffices to continue as in [34, Theorem 2]. □ We point out that the bound on $\alpha^*(p)$ can be actually improved, see [34, Theorem 2]; however, as the topic is bristly with technicalities, we avoid further technicalities and notations, sticking rather to the bounds in (28).

Next, we introduce a stabilization S_0^K satisfying the properties (24) and (25).

Theorem 7 *Given*

$$S_0^K(u_n, v_n) = \frac{h_K}{p^2}(u_n, v_n)_{0,\partial K} \quad \forall u_n,\, v_n \in \ker(\Pi_{p-1}^0),\, \forall K \in \mathcal{T}_n, \tag{29}$$

the following bounds on $\beta_*(p)$ and β^* introduced in (24) and (25), respectively, hold true:

$$\beta_*(p) \gtrsim p^{-8}, \quad \beta^* \lesssim 1.$$

Proof. We assume without loss of generality that $h_K = 1$, since the general assertion follows from a scaling argument, and that $p \geq 2$, since we are interested in the asymptotic behavior in terms of p.

We begin with the bound on $\beta_*(p)$. Given $u_n \in \ker(\Pi^0_{p-1})$, we apply the Poincaré inequality to show

$$\|u_n\|_{0,K} = \|u_n - \Pi^0_{p-1}u_n\|_{0,K} \lesssim |u_n - \Pi^0_{p-1}u_n|_{1,K},$$

where we have applied the Poincaré inequality.

Using the properties of the H^1 projector, integrating by parts, using the properties of the L^2 projector, applying the definition of the $H^{-\frac{1}{2}}(\partial K)$ norm, applying the Neumann trace inequality [99, Theorem A.33], and applying the p-inverse inequality already employed in (17), we get

$$\begin{aligned}
|u_n - \Pi^0_{p-1}u_n|^2_{1,K} &= \int_K -\Delta(u_n - \Pi^0_{p-1}u_n)(u_n - \Pi^0_{p-1}u_n) + \int_{\partial K} \partial_{\mathbf{n}}(u_n - \Pi^0_{p-1}u_n)(u_n - \Pi^0_{p-1}u_n) \\
&= \int_{\partial K} \partial_{\mathbf{n}}(u_n - \Pi^0_{p-1}u_n)(u_n - \Pi^0_{p-1}u_n) \\
&\leq \|\partial_{\mathbf{n}}(u_n - \Pi^0_{p-1}u_n)\|_{-\frac{1}{2},\partial K}\|u_n - \Pi^0_{p-1}u_n\|_{\frac{1}{2},\partial K} \\
&\lesssim \left(|u_n - \Pi^0_{p-1}u_n|_{1,K} + \|\Delta(u_n - \Pi^0_{p-1}u_n)\|_{0,K}\right)\|u_n - \Pi^0_{p-1}u_n\|_{\frac{1}{2},\partial K} \\
&\lesssim p^2|u_n - \Pi^0_{p-1}u_n|_{1,K}\|u_n - \Pi^0_{p-1}u_n\|_{\frac{1}{2},\partial K},
\end{aligned}$$

whence

$$|u_n - \Pi^0_{p-1}u_n|_{1,K} \lesssim p^2\|u_n - \Pi^0_{p-1}u_n\|_{\frac{1}{2},\partial K}.$$

Using that u_n is piecewise polynomial over ∂K and applying the one dimensional p-inverse inequality [99, Theorem 3.91] together with interpolation theory [99, Appendix B], we deduce

$$\|u_n - \Pi^0_{p-1}u_n\|_{0,K} \lesssim p^3\|u_n - \Pi^0_{p-1}u_n\|_{0,\partial K},$$

which is the claim.

For what concerns instead the fact that β^* is actually independent of p, one has

$$\|u_n - \Pi^0_{p-1}u_n\|_{0,\partial K} \leq \|u_n - \Pi^\nabla_{p-1}u_n\|_{0,\partial K} + \|\Pi^\nabla_{p-1}u_n - \Pi^0_{p-1}u_n\|_{0,\partial K}.$$

Concerning the first term on the right-hand side, we apply a Poincaré inequality; concerning the second one, we apply the p-trace inverse inequality [99, equation (4.6.4)] on every triangle in the subtriangulation $\widetilde{\mathcal{T}}_n(K)$ obtained by connecting the center of any of the maximal balls with respect to which K is star-shaped to the vertices of K, getting

$$\|u_n - \Pi^0_{p-1}u_n\|_{0,\partial K} \lesssim |u_n - \Pi^\nabla_p u_n|_{1,K} + p\|\Pi^\nabla_{p-1}u_n - \Pi^0_{p-1}u_n\|_{0,K} \lesssim p|u_n - \Pi^\nabla_{p-1}u_n|_{1,K},$$

which entails the assertion. □

The dependence in terms of p of the stability constants of S^K_1 and S^K_0 seems to be very large and plays a role also in the convergence estimates of the method, see Theorem 8. In particular, the convergence rate could be polluted by some powers of p, see for instance the estimates in Theorem 10. However:

– the dependence that we have theoretically pinpointed is in principle pessimistic. In the setting of standard (i.e., nonenhanced) VEM, such dependence was proven to be much milder in practice, see [33, Section 6.4] and [34, Section 4.1];
– also in the worst possible scenario, i.e., even assuming that the bounds on $\alpha_*(p)$ and $\alpha^*(p)$ were sharp, it is possible to show that the p- (for analytic eigenfunctions) and the hp-versions (for eigenfunctions with finite Sobolev regularity) of the method lead in any case to exponential convergence in terms of p and in the cubic root of the number of degrees of freedom, see Theorem 13 and Section 4.2, respectively.

2.4. *The virtual element method*

Having described the approximation spaces and the discrete bilinear forms, we define the method associated with the eigenvalue problem (4):

$$\begin{cases} \text{find } (\lambda_n, u_n) \in \mathbb{R} \times V_n \text{ such that } \|u_n\|_{0,\Omega} = 1 \\ a_n(u_n, v_n) + b_n(u_n, v_n) = \lambda c_n(u_n, v_n) \quad \forall v_n \in V_n. \end{cases} \tag{30}$$

The method associated with the source problem (6) is the following. Given $f \in H^1(\Omega)$,

$$\begin{cases} \text{find } u_n \in V_n \text{ such that} \\ a_n(u_n, v_n) + b_n(u_n, v_n) = c_n(f, v_n) \quad \forall v_n \in V_n. \end{cases} \tag{31}$$

The methods (30) and (31) are both well-posed thanks to the coercivity of the bilinear form on the left-hand side, which follows from (21) and (22), and the continuity of the right-hand side with respect to the $\|\cdot\|_{1,K}$-norm, see (26).

We also define the solution operator $T_n \in \mathcal{L}(H^1(\Omega))$ as

$$\mathcal{B}_n(T_n f, v_n) = c_n(f, v_n) \quad \forall v_n \in V_n,$$

where we have set $\mathcal{B}_n(\cdot,\cdot) = a_n(\cdot,\cdot) + b_n(\cdot,\cdot)$.

Analogously to the continuous case, the operator T_n is self-adjoint, compact, and positive definite. Besides, given (λ_n, w_n) an eigenmode of (30), one can prove that $(\frac{1}{\lambda_n}, w_n)$ is an eigenmode of the discrete solution operator T_n.

3. Convergence analysis of the *p*-version

This section is devoted to show the convergence of the discrete eigenfunctions and eigenvalues to the continuous ones, for the p-version of the method. A particular emphasis is stressed on the case of analytic eigenfunctions, where an exponential convergence in terms of p is proven. The exponential convergence in terms of the cubic root of the number of degrees of freedom for singular functions is not theoretically covered in the present paper, but will be the objective of a numerical investigation in Section 4.2.

The remainder of the section is organized as follows. In Section 3.1, we introduce some technical results and prove p-exponential convergence on the source problem (6) for analytic solutions; we investigate instead the approximation of the eigenvalues (with tools stemming from the Babŭska-Osborn theory) in Section 3.2.

3.1. *Some auxiliary results*

We first prove an approximation result on the continuous (6) and the discrete (31) source problems.

Theorem 8 *Given $f \in H^1(\Omega)$, let u and u_n be the solutions to the continuous and discrete source problems* (6) *and* (31)*, respectively. Then, the following bound holds true:*

$$\begin{aligned} |u - u_n|_{1,\Omega} \le{}& \mu_1(p) h_K^2 |f - \Pi^{\nabla}_{p-1} f|_{1,\mathcal{T}_n} + \mu_2(p)|u - u_I|_{1,\Omega} + \mu_3(p)|u - u_\pi|_{1,\mathcal{T}_n} \\ &+ \mu_4(p)\|u - \Pi^0_{p-1} u\|_{0,\Omega} + \mu_5(p)\|\mathbb{K}\nabla u - \Pi^0_{p-1}(\mathbb{K}\nabla u)\|_{0,\Omega} + \mu_6(p)\|Vu - \Pi^0_{p-1}(Vu)\|_{0,\Omega}, \end{aligned}$$

where

$$\begin{aligned} \mu_1(p) &= \max(\mathfrak{k}_*^{-1}, \alpha_*^{-1}(p)) \max_{K\in\mathcal{T}_n} (1 + c_P^2(K)) \max(1, \beta^*), \\ \mu_2(p) &= 1 + \max(\mathfrak{k}_*^{-1}, \alpha_*^{-1}(p)) \left[\mathfrak{k}^* + \alpha^*(p) + c_P^2(\Omega)\nu^*\right], \\ \mu_3(p) &= 4 \max(\mathfrak{k}_*^{-1}, \alpha_*^{-1}(p)) \left[\mathfrak{k}^* + \alpha^*(p)\right], \\ \mu_4(p) &= 2(\mathfrak{k}_* + \alpha_*(p)) c_P(\Omega)\nu^* \\ \mu_5(p) &= 2 \max(\mathfrak{k}_*^{-1}, \alpha_*^{-1}(p)), \\ \mu_6(p) &= 2c_P^2(\Omega) \max(\mathfrak{k}_*^{-1}, \alpha_*^{-1}(p)), \end{aligned}$$

being $\alpha_*(p)$ and $\alpha^*(p)$ defined in (20)*, β^* being defined in* (25)*, $\mathfrak{k}_*$ and $\mathfrak{k}^*$ being defined in* (1)*, and ν^* being defined in* (2)*, and having set $\Pi^0_{p-1}(u)_{|K} = \Pi^{0,K}_{p-1}(u_{|K})$ and $\Pi^{\nabla}_p(u)_{|K} = \Pi^{\nabla,K}_p(u_{|K})$.*

Proof. Setting $\delta_n = u_n - u_I$, we apply (21), we use the positiveness of b_n in (22), and we perform some computations, getting

$$\begin{aligned}\min(\mathfrak{k}_*, \alpha_*(p))|\delta_n|_{1,\Omega}^2 &\le a_n(\delta_n,\delta_n) \le a_n(\delta_n,\delta_n) + b_n(\delta_n,\delta_n)\\ &= a_n(u_n,\delta_n) + b_n(u_n,\delta_n) - \sum_{K\in\mathcal{T}_n}\{a_n^K(u_I,\delta_n) + b_n(u_I,\delta_n)\}.\end{aligned}$$

We note that, for all $K \in \mathcal{T}_n$,

$$\begin{aligned}a_n^K(u_I,\delta_n) + b_n(u_I,\delta_n) &= a_n^K(u_I-u_\pi,\delta_n) + a_n^K(u_\pi - u,\delta_n) + a_n^K(u,\delta_n) - a^K(u,\delta_n)\\ &\quad + a^K(u,\delta_n) + b^K(u,\delta_n) + b_n^K(u_I-u,\delta_n) + b_n^K(u,\delta_n) - b^K(u,\delta_n).\end{aligned}$$

Thus, recalling (6) and (31), we obtain

$$\begin{aligned}\min(\mathfrak{k}_*, \alpha_*(p))|\delta_n|_{1,\Omega}^2 \le& \underbrace{c_n(f,\delta_n) - c(f,\delta_n)}_{A}\\ &- \sum_{K\in\mathcal{T}_n}\{\underbrace{a_n^K(u_I-u_\pi,\delta_n)}_{B^K} + \underbrace{a_n^K(u_\pi-u,\delta_n)}_{C^K} + \underbrace{a_n^K(u,\delta_n) - a^K(u,\delta_n)}_{D^K}\\ &\qquad + \underbrace{b_n^K(u_I-u,\delta_n)}_{E^K} + \underbrace{b_n^K(u,\delta_n) - b^K(u,\delta_n)}_{F^K}\}.\end{aligned} \tag{32}$$

We bound the six terms on the right-hand side of (32) separately.

We begin with the first one. Applying the definitions of c_n and c in (5) and (23), respectively, using (25) and the properties of the L^2 projector, and applying a Poincaré inequality, we deduce

$$\begin{aligned}&= c_n(f,\delta_n) - c(f,\delta_n) = \sum_{K\in\mathcal{T}_n}\left((\Pi_{p-1}^0 f, \Pi_{p-1}^0\delta_n)_{0,K} + S_0^K((I-\Pi_{p-1}^0)f,(I-\Pi_{p-1}^0)\delta_n) - (f,\delta_n)_{0,K}\right)\\ &\le \sum_{K\in\mathcal{T}_n}\left(h_K^2\beta^*|f-\Pi_{p-1}^\nabla f|_{1,K}|\delta_n - \Pi_p^\nabla\delta_n|_{1,K} + \|f-\Pi_{p-1}^0 f\|_{0,K}\|\delta_n - \Pi_{p-1}^0\delta_n\|_{0,K}\right)\\ &\le \sum_{K\in\mathcal{T}_n}(1+c_P^2(K))\max(1,\beta^*)h_K^2|f-\Pi_{p-1}^\nabla f|_{1,K}|\delta_n-\Pi_{p-1}^\nabla\delta_n|_{1,K}\\ &\le \sum_{K\in\mathcal{T}_n}(1+c_P^2(K))\max(1,\beta^*)h_K^2|f-\Pi_{p-1}^\nabla f|_{1,K}|\delta_n|_{1,K},\end{aligned}$$

where $c_P(K)h_K$ denotes the Poincaré constant over the element K.

Next, we concentrate on the second local term. Thanks to Lemma 4, we have

$$\begin{aligned}B^K = a_n^K(u_I-u_\pi,\delta_n) &\le (\mathfrak{k}^* + \alpha^*(p))|u_I-u_\pi|_{1,K}|\delta_n|_{1,K}\\ &\le (\mathfrak{k}^* + \alpha^*(p))(|u-u_I|_{1,K} + |u-u_\pi|_{1,K})|\delta_n|_{1,K}.\end{aligned}$$

For what concerns the third local term, Lemma 4 again yields

$$C^K = a_n^K(u_\pi - u,\delta_n) \le (\mathfrak{k}^* + \alpha^*(p))|u-u_\pi|_{1,K}|\delta_n|_{1,K}.$$

Regarding the fourth local term, we apply the definition of (5) and (19), respectively, the properties of the L^2 projector, (1), and (20), getting

$$\begin{aligned}D^K &= a_n^K(u,\delta_n) - a^K(u,\delta_n)\\ &= (\mathbb{K}\Pi_{p-1}^0\nabla u, \Pi_{p-1}^0\nabla\delta_n)_{0,K} + S_1^K((I-\Pi_p^\nabla)u,(I-\Pi_p^\nabla)\delta_n) - (\mathbb{K}\nabla u,\nabla\delta_n)_{0,K}\\ &= (\mathbb{K}(\Pi_{p-1}^0\nabla u - \nabla u), \Pi_{p-1}^0\nabla\delta_n)_{0,K} - (\mathbb{K}\nabla u - \Pi_{p-1}^0(\mathbb{K}\nabla u), \nabla\delta_n - \Pi_{p-1}^0\nabla\delta_n)_{0,K}\\ &\quad + S_1^K((I-\Pi_p^\nabla)u,(I-\Pi_p^\nabla)\delta_n)\\ &\le \left(\mathfrak{k}^*\|\nabla u - \Pi_{p-1}^0\nabla u\|_{0,K} + \|\mathbb{K}\nabla u - \Pi_{p-1}^0(\mathbb{K}\nabla u)\|_{0,K} + \alpha^*(p)|u-\Pi_p^\nabla u|_{1,K}\right)|\delta_n|_{1,K}.\end{aligned}$$

The fifth local term can be bounded using (2) and (22):

$$E^K = b_n^K(u_I-u,\delta_n) \le \nu^*\|u-u_I\|_{0,K}\|\delta_n\|_{0,K}.$$

Eventually, we deal with the sixth local term, which can be bounded employing the definitions of b_n^K and b_n in (5) and (22), respectively, and (2).

$$\begin{aligned} F^K = b_n^K(u,\delta_n) - b^K(u,\delta_n) &= (V\Pi_{p-1}^0 u, \Pi_{p-1}^0\delta_n)_{0,K} - (Vu,\delta_n)_{0,K} \\ &= (V(\Pi_{p-1}^0 u - u), \Pi_{p-1}^0\delta_n)_{0,K} - (Vu, \delta_n - \Pi_{p-1}^0\delta_n)_{0,K} \\ &\leq (\nu^*\|u - \Pi_{p-1}^0 u\|_{0,K} + \|Vu - \Pi_{p-1}^0 Vu\|_{0,K})\|\delta_n\|_{0,K}. \end{aligned}$$

Collecting the six bounds above in (32), applying an ℓ^2 Cauchy-Schwarz inequality, and applying a Poincaré inequality on Ω (with constant $c_P(\Omega)$), yields

$$\begin{aligned} \min(\mathfrak{k}_*, \alpha_*(p))|\delta_n|_{1,\Omega} \leq \max_{K\in\mathcal{T}_n}(1 + c_P^2(K))\max(1,\beta^*)h_K^2|f - \Pi_{p-1}^\nabla f|_{1,\mathcal{T}_n} \\ + (\mathfrak{k}^* + \alpha^*(p))(|u - u_I|_{1,\Omega} + 2|u - u_\pi|_{1,\mathcal{T}_n}) \\ + 2\mathfrak{k}^*\|\nabla u - \Pi_{p-1}^0\nabla u\|_{0,\mathcal{T}_n} + 2\|\mathbb{K}\nabla u - \Pi_{p-1}^0(\mathbb{K}\nabla u)\|_{0,\Omega} + 2\alpha^*(p)|u - u_\pi|_{1,\mathcal{T}_n} \\ + c_P^2(\Omega)\nu^*|u - u_I|_{0,\Omega} + 2c_P(\Omega)\nu^*\|u - \Pi_{p-1}^0 u\|_{0,\Omega} + 2c_P^2(\Omega)\|Vu - \Pi_{p-1}^0(Vu)\|_{0,\Omega}. \end{aligned}$$

The assertion follows by noting that

$$|u - u_n|_{1,\Omega} \leq |u - u_I|_{1,\Omega} + |\delta_n|_{1,\Omega}.$$

□ We can simplify the estimates of Theorem 8 as follows.

Corollary 9 *Given $f \in H^1(\Omega)$, let u and u_n be the solutions to* (6) *and* (31)*, respectively. Then, the following bound holds true:*

$$\begin{aligned} |u - u_n|_{1,\Omega} \lesssim \frac{1}{\min(\mathfrak{k}_*, \alpha_*(p))}\big\{&\max(1,\beta^*)^* h_K^2|f - \Pi_{p-1}^\nabla f|_{1,\mathcal{T}_n} \\ &+ (\mathfrak{k}^* + \alpha^*(p))(|u - u_I|_{1,\Omega} + |u - u_\pi|_{1,\mathcal{T}_n} + \|u - \Pi_{p-1}^0 u\|_{0,\Omega}) \\ &+ \|\mathbb{K}\nabla u - \Pi_{p-1}^0(\mathbb{K}\nabla u)\|_{0,\Omega} + \|Vu - \Pi_{p-1}^0(Vu)\|_{0,\Omega}\big\}, \end{aligned}$$

being $\alpha_*(p)$ and $\alpha^*(p)$ defined in (20)*, and β^* being defined in* (25)*.*

Therefore, best polynomial approximation and best interpolation results entail the following theorem, which states the convergence rate of the error in the approximation of the source problem (6).

Theorem 10 *Let u and f the solution and the right-hand side of problem* (6) *belong to $H^1(\Omega)$, and let their restriction on every element $K \in \mathcal{T}_n$ belong to $H^{s+1}(K)$, $s \geq 0$. Then, recalling that the coefficients $\mathbb{K}$ and V in* (6) *are piecewise analytic over $\mathcal{T}_n$, see assumption (**A**), it holds that*

$$|u - u_n|_{1,\Omega} \lesssim \frac{\max(1, \mathfrak{k}^* + \alpha^*(p), \beta^*)}{\min(\mathfrak{k}_*, \alpha_*(p))}\frac{h^{\min(p,s)}}{p^{s-1}}\left(h^2\|f\|_{s+1,\mathcal{T}_n} + \|u\|_{s+1,\mathcal{T}_n} + \|Vu\|_{s+1,\mathcal{T}_n} + \|\mathbb{K}\nabla u\|_{s,\mathcal{T}_n}\right).$$

Proof. It suffices to combine Theorem 1, Corollary 3, and Corollary 9. □

It is clear from the estimate in Theorem 10 that, whereas the h-version of the method converges optimally, the p-version, whenever u, the solution to problem (6), has finite Sobolev regularity, does not. On the one hand, we showed in Corollary 3 that in the enhanced VEM framework, the best interpolation estimates are suboptimal of one power, see Corollary 3; on the other, one also has to pay additional powers of p due to the effects of the local stabilizations S_1^K and S_0^K.

At any rate, if u is the restriction on Ω of an analytic solution, the rate of convergence in terms of p, is exponential, as stated in the following result.

Theorem 11 *Let u, the solution to the source problem* (6)*, be the restriction on Ω of an analytic function defined on a sufficiently large extension of Ω. Then,*

$$|u - u_n|_{1,\Omega} \lesssim \exp(-b\,p),$$

for some positive constant b independent of the discretization parameters.

Proof. Having at disposal Theorem 10, it suffices to apply the argument of [33, Section 5]. □ On of the main point behind the proof of Theorem 11 is that the algebraic losses in terms of p, due to the suboptimality

of the best interpolation estimates and to the presence of the stabilizing parameters $\alpha_*(p)$ and $\alpha^*(p)$, are absorbed in a term which is exponentially decreasing in p.

It still remains open the issue of how to proceed in case the solution is not analytic, if one wants to have again an optimal convergence of the error. In fact, the instance of finite Sobolev regularity solutions will be numerically addressed in Section 4, where the *hp*-version of the method will be considered, and exponential convergence in terms of the cubic root of the number of degrees of freedom will be shown. A theoretical analysis of this approach is actually possible, e.g. following the lines of [34, Section 5], but is not addressed in the present paper.

In the remainder of Section 3, we assume therefore that u fulfills the assumptions of Theorem 11. Moreover, we will focus on the p-version only, since the h-analysis was the topic of [60].

3.2. *p-spectral approximation for compact operators*

We proceed now with the convergence analysis of the eigenfunctions and the eigenvalues of the solution operator T. We will employ the tools of the Babŭska-Osborn theory for compact operators [18].

More precisely, given T the solution operator associated with the problem (6), and T_n, the sequence of compact solution operators associated with the method (31), the condition

$$\|T - T_n\|_{\mathcal{L}(H^1(\Omega))} \longrightarrow 0 \quad \text{as} \quad n \longrightarrow +\infty, \tag{33}$$

is sufficient [18, 41] in order to get the two following facts.

Assuming that h and p are sufficiently small and large, respectively,

– given λ an exact eigenvalue in (4) with multiplicity m, method (30) provides precisely m discrete eigenvalues converging to λ;
– given λ_n a discrete eigenvalue, λ_n converges to a continuous eigenvalue.

Importantly, the condition (33) is also necessary in order to prove spectral approximation properties, see [42].

Thus, we begin with the following result, which provides (33) for the p-version of VEM, in case the solution to the source problem (6) is the restriction of an analytic solution over a sufficiently large extension of the domain Ω. We underline once again that the case of nonanalytic eigenfunctions will be numerically addressed in Section 4, with the aid of the *hp*-version of the method.

Lemma 12 *Under the assumptions of Theorem 11, it holds that*

$$\|T - T_n\|_{\mathcal{L}(H^1(\Omega))} \lesssim \exp(-b\,p),$$

for some positive constant b independent of the discretization parameters.

Proof. It suffices to observe that

$$\begin{aligned}\|T - T_n\|_{\mathcal{L}(H^1(\Omega))} &= \sup_{f\in H^1(\Omega),\|f\|_{1,\Omega}=1} \|Tf - T_n f\|_{1,\Omega} = \sup_{f\in H^1(\Omega),\|f\|_{1,\Omega}=1} \|u - u_n\|_{1,\Omega} \\ &\leq (1 + c_P(\Omega)) \sup_{f\in H^1(\Omega),\|f\|_{1,\Omega}=1} |u - u_n|_{1,\Omega},\end{aligned}$$

where $c_P(\Omega)$ is the Poincaré constant on Ω, and then apply Theorem 11. □ The convergence rate for eigenfunctions is a consequence of Lemma 12 and the Babŭska-Osborn theory. In particular, given λ a continuous eigenvalue with multiplicity m, and given $\lambda_{1,n}, \ldots, \lambda_{m,n}$ the associated discrete eigenvalues, we first define the gap between $\mathcal{E}_{\lambda,n}$, which is the direct sum of the eigenspaces generated by $\lambda_{1,n}, \ldots, \lambda_{m,n}$, and $\mathcal{E}_\lambda$, which is the eigenspace generated by λ:

$$\widehat{\delta}(\mathcal{E}_\lambda, \mathcal{E}_{\lambda,n}) = \max\left(\delta(\mathcal{E}_\lambda, \mathcal{E}_{\lambda,n}), \delta(\mathcal{E}_{\lambda,n}, \mathcal{E}_\lambda)\right), \tag{34}$$

where

$$\delta(\mathbf{X}, \mathbf{Y}) = \sup_{x\in\mathbf{X},\, \|x\|_{0,\Omega}=1} \left(\inf_{y\in\mathbf{Y}} \|x - y\|_{1,\Omega}\right).$$

The following bound on the gap $\widehat{\delta}(\mathcal{E}_\lambda, \mathcal{E}_{\lambda,n})$ is valid.

Theorem 13 *Under the assumptions of Theorem 11, it holds true that*

$$\widehat{\delta}(\mathcal{E}_\lambda, \mathcal{E}_{\lambda,n}) \lesssim \exp(-bp),$$

for some positive constant b independent of the discretization parameters.
Proof. Having at disposal Lemma 12, the assertion is an application of the Babŭska-Osborn theory [18, Theorem 7.1 and 7.3]. □

Remark 3 *Owing to the definition* (34)*, Theorem 13 entails the p-exponential convergence of the eigenfunctions.*
Finally, we address the convergence of the eigenvalues.
Theorem 14 *Under the assumptions of Theorem 11, let λ_n be an eigenvalue of the discrete solution operator T_n, associated with the eigenvalue λ of the continuous solution operator T. Then, it holds true that*

$$|\lambda_n - \lambda| \lesssim \exp(-b\,p),$$

for some positive constant b independent of the discretization parameters.
Proof. The proof follows the line e.g. of that of [94, Theorem 4.3]. Let w_n be a discrete eigenfunction associated with the discrete eigenvalue λ_n, and let w and λ be the corresponding exact eigenfunction and eigenvalue, respectively. Then, one has

$$\begin{aligned}
&a(w-w_n, w-w_n) + b(w-w_n, w-w_n) - \lambda c(w-w_n, w-w_n) \\
&= a(w_n, w_n) + b(w_n, w_n) - \lambda c(w_n, w_n) \\
&= a(w_n, w_n) + b(w_n, w_n) - a_n(w_n, w_n) - b_n(w_n, w_n) + \lambda_n c_n(w_n, w_n) - \lambda c(w_n, w_n).
\end{aligned}$$

Noting that

$$\lambda_n c_n(w_n, w_n) - \lambda c(w_n, w_n) = \lambda_n \left(c_n(w_n, w_n) - c(w_n, w_n)\right) + (\lambda_n - \lambda) c(w_n, w_n),$$

we deduce

$$\begin{aligned}
(\lambda_n - \lambda) c(w_n, w_n) = {} & a(w-w_n, w-w_n) + b(w-w_n, w-w_n) - \lambda c(w-w_n, w-w_n) \\
& + a_n(w_n, w_n) - a(w_n, w_n) + b_n(w_n, w_n) - b(w_n, w_n) \\
& - \lambda_n \left[c_n(w_n, w_n) - c(w_n, w_n)\right].
\end{aligned}$$

The assertion follows by bounding the terms on the right-hand side (with tools similar to those employed in the proof of Theorem 8) and then using the convergence of the eigenfunctions discussed in Remark 3. □ We

note that in the standard h-analysis of the convergence of the eigenvalues one typically gets a double rate of convergence. Since here we are focusing on the p-version on the case of eigenfunctions being the restriction of analytic functions only, the double rate of convergence is actually hidden within the exponential convergence rate.

4. Numerical results

In this section, we present a number of numerical experiments that validate the exponential convergence in terms of the degree of accuracy p of the discrete eigenvalues to the continuous ones, whenever the corresponding eigenfunctions are the restriction over the physical domain of analytic functions, see Section 4.1. Instead, in Section 4.2, we tackle the instance of eigenfunctions possibly having finite Sobolev regularity, by means of the hp-version of the method, and we show that the discrete eigenvalues converge to the continuous ones exponentially in terms of the cubic root of the number of degrees of freedom.

In particular, we are interested in the convergence rate of the normalized error

$$\frac{|\lambda - \lambda_n|}{|\lambda|}, \tag{35}$$

where λ is a continuous eigenvalues in (4) and λ_n is a discrete eigenvalue in (30) associated with λ.

In the forthcoming numerical experiments, we could employ the stabilizations introduced in Section 2.3.1. The reason why we picked S_1^K and S_0^K in (27) and (29), respectively, is that we can prove explicit bounds in terms of the "polynomial" degree p on the parameters $\alpha_*(p)$, $\alpha^*(p)$, $\beta_*(p)$, and β^*. A possible effective alternative to S_1^K is provided by the so-called diagonal-recipe stabilizations, defined as

$$\widetilde{S}_1^K(\varphi_j, \varphi_i) = \max(1, a^K(\Pi_p^\nabla \varphi_i, \Pi_p^\nabla \varphi_j))\delta_{i,j}, \tag{36}$$

where we recall that $\{\varphi_i\}_{i=1}^{\dim(V_n(K))}$ is the canonical basis of $V_n(K)$, and where $\delta_{i,j}$ denotes the Kronecker delta.

Such stabilization was introduced in [35] and its performance was investigated in [91] and [65] in the approximation of a 2D and a 3D Poisson problem, respectively. If compared to other stabilizing bilinear forms, it entails more robust performance of the method for high "polynomial" degree and in presence of distorted or with bad aspect ratio elements. For this reason, we will employ $\widetilde{S}_1^K$ in (36) and S_0^K in (29) as stabilizations for the method.

For what concerns the choice of the polynomial basis $\{m_\alpha\}_{\alpha=1}^{\pi_{p-2}}$ dual to the internal moments (11), we fix an $L^2(K)$ orthonormal basis elementwise. In fact, as analyzed in [91], this choice is particularly effective when the "polynomial" degree of the method is high and when the elements are distorted and/or have a bad aspect ratio.

4.1. *p-version: the case of analytic eigenfunctions*

In this section, we fix our attention to the performance of the p-version of the method in the case of analytic eigenfunctions.

Test case 1: Laplace on square domain. As a first test case, we consider as a physical domain the unit square $\Omega_1 = (0,1)^2$, partitioned into sequences of Voronoi meshes, see e.g. [96].

We approximate the eigenvalues of the Laplace operator on Ω_1, i.e., we pick $\mathbb{K} = \mathbb{I}$ (that is, the identity matrix) and $V = 0$ in (3). The eigenvalues are explicitly known and are given by $\lambda_{k_1,k_2} = (k_1^2 + k_2^2)\pi^2$ for all k_1 and k_2 in $\mathbb{N}$ such that $k_1 + k_2 \neq 0$.

From Theorem 14 and from Remark 3, since all the eigenfunctions are the restriction of analytic functions over $\mathbb{R}^2$, as they have the form $\sin(\pi x)\sin(\pi y)$ for all k_1 and k_2 in $\mathbb{N}$ such that $k_1 + k_2 \neq 0$, the discrete eigenvalues converge exponentially in terms of p, and therefore in terms of the square root of the number of degrees of freedom, to the continuous ones.

In Figure 1, we plot the error (35) against the square root of the number of degrees of freedom, cf. Theorem (14), for the first four eigenvalues. We employ the h-version for $p = 1$, 2, and 3, and the p-version of the method. On the x-axis, we plot the square root of the number of degrees of freedom.

Test case 2: quantum harmonic oscillator on a square. Another interesting test case with analytic eigenfunctions is provided by the quantum harmonic oscillator [81, 84], that is, when one fixes $\mathbb{K} = 0.5\mathbb{I}$ (that is, again, the identity matrix) and $V(x,y) = 0.5(x^2 + y^2)$ in (3). The eigenfunctions on $\mathbb{R}^2$ are given by the product of the Gaussian bell $\exp(-(x^2 + y^2))$ with a tensor product of Hermite polynomials. The eigenvalues are all the natural numbers; every eigenvalue $n \in \mathbb{N}$ has multiplicity precisely equal to n.

The eigenfunctions of the quantum harmonic oscillator have not zero boundary conditions on bounded domains; however, they decrease rapidly to zero as x and y tend to infinity. For this reason, we consider as a physical domain, the (sufficiently wide) square $\Omega_2 = (-10, 10)^2$, and we impose zero boundary conditions, assuming that the resulting eigenfunctions and eigenvalues are practically given by those in the unbounded domain $\mathbb{R}^2$. Again, we compare the performance of the h-version with $p = 1$, 2, and 3 with the p-version of the method on Voronoi meshes. On the x-axis, we consider the square root of the number of degrees of freedom, which we recall is a consequence of Theorem 14.

In Figure 2, one can appreciate the exponential decay of the error in terms of the square root of the number of degrees of freedom.

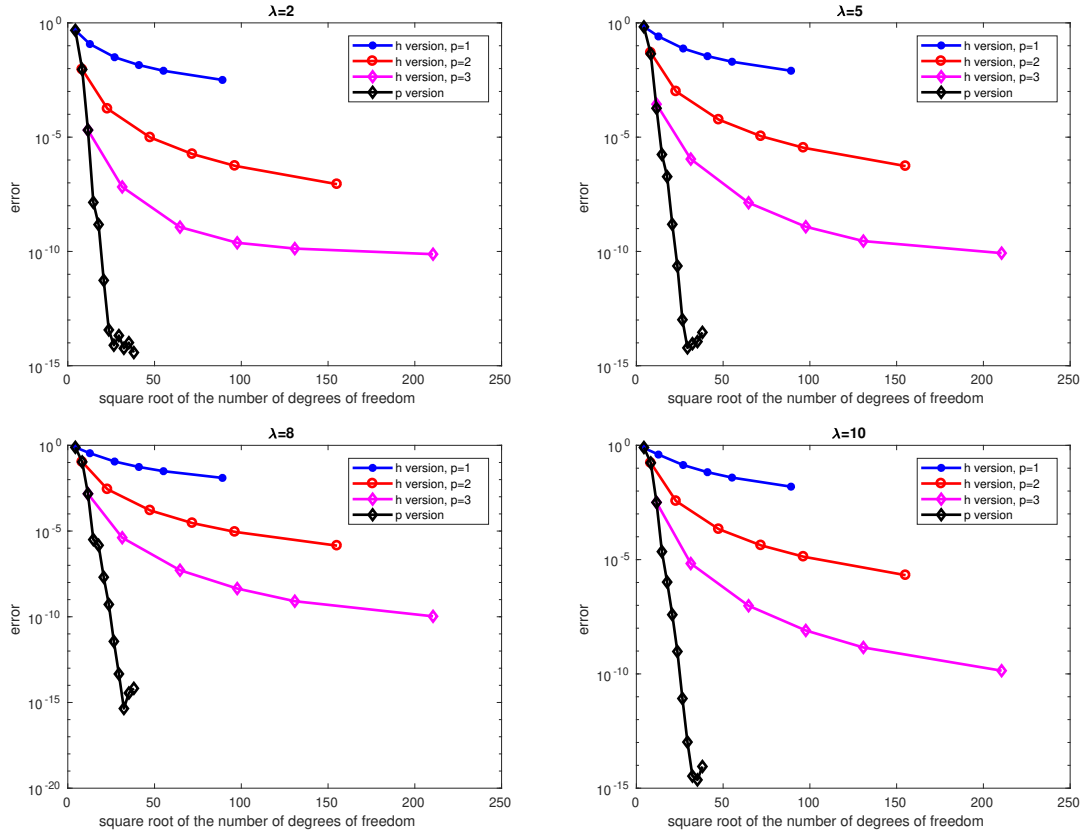

Fig. 1. Convergence of the error (35) for the first four distinct Dirichlet eigenvalues of the Laplace operator on the square domain Ω_1 employing the h-version with $p = 1$, 2, and 3 and the p-version of the method. On the x-axis, we plot the square root of the number of degrees of freedom. The stabilizations $\widetilde{S}_1^K$ and S_0^K are defined in (36) and (29), respectively. The polynomial basis dual to the internal moments (11) is L^2 orthonormal elementwise. For both the h- and the p-versions, we employ Voronoi meshes. The error curves plotted in the figure refer to the approximation of the problem eigenvalues as follows: *top-left panel:* first eigenvalue; *top-right panel:* second eigenvalue; *bottom-left panel:* third eigenvalue; *bottom-right panel:* fourth eigenvalue.

4.2. *hp-version: the case of singular eigenfunctions*

This section is devoted to the approximation of eigenfunctions that are not analytic, but rather could present some singularities. For the sake of simplicity, we consider test cases where the singularities are concentrated at isolated points only; for instance, we avoid the more technical case of edge singularities, where anisotropic mesh refinements could come into play.

In Section 3, we analyzed the convergence rate of the method and we underlined the suboptimality of the p-version for nonanalytic eigenfunctions, see Theorem 10 and the comments below. In particular, the bound in Theorem 10, together with the stray behavior in terms of p of the stability constants $\alpha_*(p)$ and $\alpha^*(p)$, could lead in principle also to a divergent method for eigenfunctions with sufficiently strong singularities.

Thus, we resort to the *hp*-version of the method, which will be described in the forthcoming Section 4.2.1. Such a strategy follows the line of the construction in [17, 34, 99]; by a proper combination of local mesh refinements and increasing the number of the "polynomial" degree over the polygonal decomposition in a nonuniform way, is possible to recover exponential convergence of the method in terms of the cubic root of the number of degrees of freedom.

A couple of test cases dealing with the *hp*-version of the method will be presented in Section 4.2.2.

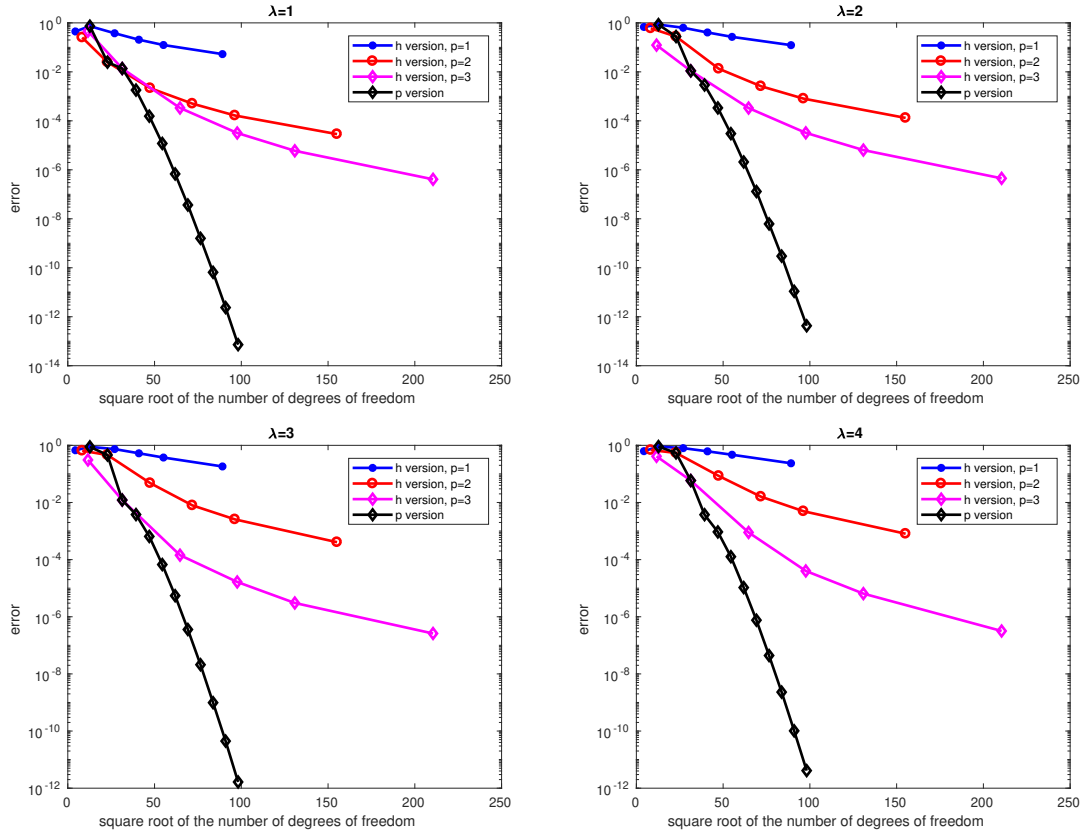

Fig. 2. Convergence of the error (35) for the first four distinct Dirichlet eigenvalues of the quantum harmonic oscillator operator on the square domain Ω_2 employing the h-version with $p = 1$, 2, and 3 and the p-version of the method. On the x-axis, we plot the square root of the number of degrees of freedom. The stabilizations $\widetilde{S}_1^K$ and S_0^K are defined in (36) and (29), respectively. The polynomial basis dual to the internal moments (11) is L^2 orthonormal elementwise. For both the h- and the p-versions, we employ Voronoi meshes. The error curves plotted in the figure refer to the approximation of the problem eigenvalues as follows: *top-left panel:* first eigenvalue; *top-right panel:* second eigenvalue; *bottom-left panel:* third eigenvalue; *bottom-right panel:* fourth eigenvalue.

4.2.1. *hp-virtual element spaces*

In this section, we describe the structure of *hp*-virtual element space, which will be instrumental for the approximation of eigenfunctions with finite Sobolev regularity, see Section 4.2.2.

The idea behind the *hp*-refinements is that geometric mesh refinements are performed on the elements where the solution of the target problem is singular, whereas p-refinements are performed on the elements where the solution is analytic. Henceforth, we assume for the sake of simplicity that the eigenfunctions are analytic everywhere in Ω, but at a set $\mathcal{M}$ of M points, lying either in the interior of Ω or on its boundary.

As a first step in this construction, we introduce the concept of layers associated with $\mathcal{M}$ of a sequence of meshes $\{\mathcal{T}_n\}_{n\in\mathbb{N}}$. Given $n \in \mathbb{N}$, we assume that the mesh $\mathcal{T}_n$ consists of $n+1$ layers, where the 0-th layer L_0^n consists of all the elements abutting the points in $\mathcal{M}$. The other layers are defined by induction as

$$L_j^n = \left\{ K_1 \in \mathcal{T}_n \mid \overline{K_1} \cap \overline{K_2} \neq \emptyset \text{ for some } K_2 \in L_{j-1}^n,\ K_1 \notin \cup_{i=0}^{j-1} L_i^n \right\} \quad \forall j = 1, \ldots, n.$$

Next, we introduce the concept of geometrically graded meshes $\{\mathcal{T}_n\}_{n\in\mathbb{N}}$. For all $n \in \mathbb{N}$, there exists a (grading) parameter $\sigma \in (0, 1)$ such that

$$h_K \approx \sigma^{n-j} \quad \text{in } K \in L_j^n.$$

Therefore, geometrically graded meshes are characterized by very "tiny" elements abutting the "singular" points in $\mathcal{M}$, and by elements increasing their size geometrically, when increasing the index of the layer

they belong to. Roughly speaking, the "tiny" elements guarantee good approximation properties where the target function is singular. In Figures 3 and 5, we have depicted the first three meshes of two sequences of geometric graded meshes; we have highlighted different layers in different colors.

The local "polynomial" degrees are distributed in a nonuniform way. More precisely, we fix a parameter $\mu \in \mathbb{N}$ and define a vector $\mathbf{p} \in \mathbb{N}^{\mathrm{card}(\mathcal{T}_n)}$, such that

$$\mathbf{p}_\ell = \mu(j+1) \quad \text{if} \quad K_\ell \in L_j^n \quad \forall \ell = 1, \dots, \mathrm{card}(\mathcal{T}_n). \tag{37}$$

The idea behind this choice is that the local "polynomial" degree of the method on $V_n(K)$ increases linearly when increasing the layer index. This is sufficient in standard *hp*-methods [17, 34, 99] to get exponential convergence in terms of the cubic root of the number of degrees of freedom.

Next, we construct another vector $\mathbf{p}_{\mathcal{E}} \in \mathbb{N}^{\mathrm{card}(\mathcal{E}_n)}$, whose entries are defined by

$$\mathbf{p}_{\mathcal{E}\widetilde{\ell}} = \begin{cases} \max(\mathbf{p}_{\ell_1}, \mathbf{p}_{\ell_2}) & \text{if } e_{\widetilde{\ell}} \in \mathcal{E}_n^I \text{ and } e_{\widetilde{\ell}} \subseteq \partial K_{\ell_1} \cap \partial K_{\ell_2} \\ \mathbf{p}_\ell & \text{if } e_{\widetilde{\ell}} \in \mathcal{E}_n^B \text{ and } e_{\widetilde{\ell}} \subset \partial K_\ell, \end{cases} \tag{38}$$

where we recall that $\mathcal{E}_n^B$ and $\mathcal{E}_n^I$ denote the set of boundary and internal edges of $\mathcal{T}_n$, respectively.

The *hp*-virtual element spaces are consequently defined by considering the Laplacian in the space of polynomials of degree p_ℓ on the element K_ℓ, for all $\ell = 1, \dots, \mathrm{card}(\mathcal{T}_n)$, fixing piecewise continuous polynomial Dirichlet traces over the edges with degree chosen accordingly to the maximum rule (38), and then imposing the enhancing constraints locally as in (10).

Following the lines of [34, Section 5], it is possible to prove that, employing the *hp*-spaces, the error $|u - u_n|_{1,\Omega}$ converges exponentially in terms of the cubic root of the number of degrees of freedom, also if the estimates in Theorem 10 are severely suboptimal in p. The important point when trying to recover exponential convergence is that the suboptimal factor haunting the *hp*-version of the VEM grows at most algebraically in p.

Since the matter is technical and follows broadly by combining the techniques of [34] and the results in Section 3, we limit ourselves to present here the numerical results. As an interesting side remark, we underline that so far the construction of the *hp*-strategy was based on a priori knowledge of the singular behavior of the eigenfunctions. One could also build *hp*-spaces in an adaptive fashion, employing for instance residual-based a posteriori error analysis, as done in [37].

4.2.2. *Numerical experiments*

In this section, we present numerical experiments on a couple of test cases where the eigenfunctions have (possibly) finite Sobolev regularity, at some isolated points. In particular, we compare the performance of the *h*- and of the *hp*-versions. In the first test case, the singular behavior is due to the shape of the physical domain, which is assumed to be L-shaped. In the second, it is instead due to the discontinuity of the diffusivity tensor $\mathbb{K}$; namely, we will consider the so-called *checkerboard benchmark*, see e.g. [61].

The *h*-version is performed always employing uniform Cartesian meshes. In the checkerboard case, the Cartesian meshes are assumed to be conforming with respect to the discontinuities of the diffusivity tensor. We also underline that the construction of *hp*-spaces benefit from the possibility of using polygonal meshes, see Figures 3 and 5.

Test case 3: Laplace on L-shaped domain. In this test case, we fix as a physical domain, the L-shaped domain $\Omega_3 = (-1,1)^2 \setminus (-1,0]^2$. We look for eigenvalues of the Laplace operator; thus, we set $\mathbb{K} = \mathbb{I}$ (that is, the identity matrix) and $V = 0$ in (3). For what concerns the *hp*-version, we consider a distribution of the "polynomial" degrees as in (37), picking $\mu = 1$. We consider here homogeneous Neumann boundary conditions; note that the method when imposing Neumann boundary conditions is defined similarly to (30), see e.g. [12, Remark 2.2].

The geometrically graded meshes are built by taking as a grading parameter $\sigma = 0.5$, the geometric refinement is towards the re-entrant corner. The first three meshes, together with the corresponding distribution of the "polynomial" degrees, are depicted in Figure 3.

In order to test the method, we compare our discrete eigenvalues with those described in Dauge's website [66]. The numerical results, describing the convergence to the first four distinct eigenvalues when em-

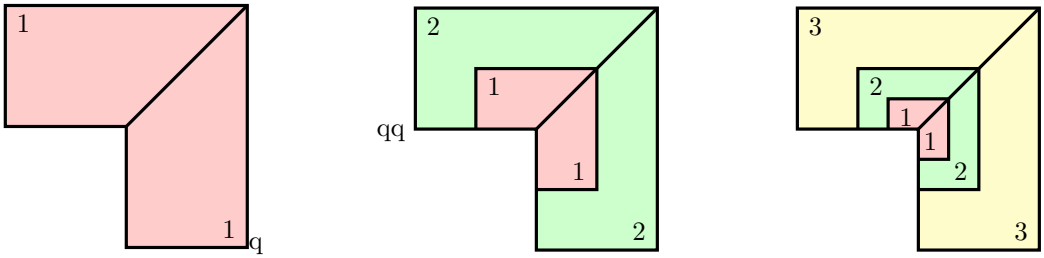

Fig. 3. First three meshes $\mathcal{T}_0$, $\mathcal{T}_1$, and $\mathcal{T}_2$, and the distribution of the "polynomial" degree for the approximation of eigenfunctions and eigenvalues of the Laplace operator on the L-shaped domain Ω_3. The 0-th, the 1-st, and the 2-nd layers are highlighted in red, green, and yellow colors, respectively. The layers are constructed refining only towards the reentrant corner.

ploying the *h*- and the *hp*-versions of the method on a sequence of uniform Cartesian meshes and on the sequence of graded meshes in Figure 3, are depicted in Figure 4.

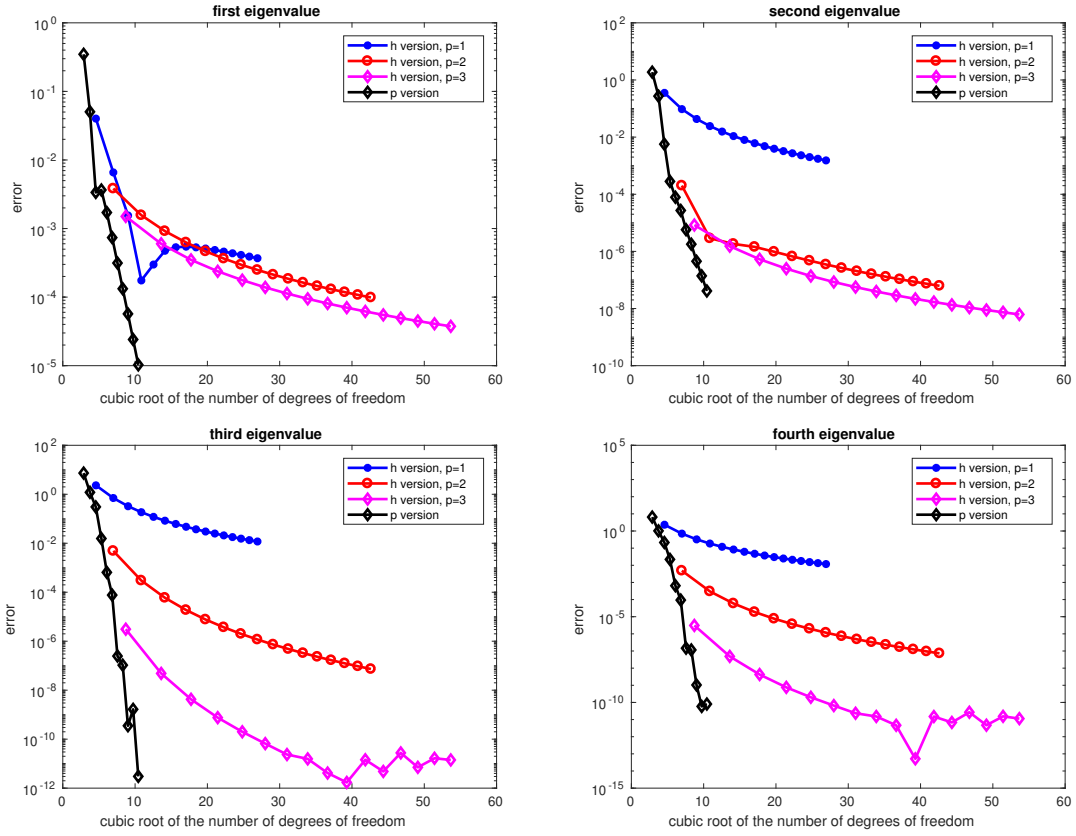

Fig. 4. Convergence of the error (35) for the first four distinct Neumann eigenvalues of the Laplace operator on the L-shaped domain Ω_3 employing the *h*-version with $p = 1$, 2, and 3 and the *hp*-version of the method. On the x-axis, we plot the cubic root of the number of degrees of freedom. The stabilizations $\widetilde{S}_1^K$ and S_0^K are defined in (36) and (29), respectively. The polynomial basis dual to the internal moments (11) is L^2 orthonormal elementwise. For the *h*-version we employ uniform Cartesian meshes, for the *p*-versions, we employ the meshes in Figure 3. The error curves plotted in the figure refer to the approximation of the problem eigenvalues as follows: *top-left panel:* first eigenvalue; *top-right panel:* second eigenvalue; *bottom-left panel:* third eigenvalue; *bottom-right panel:* fourth eigenvalue.

From Figure 4, it is possible to appreciate the exponential convergence of the *hp*-version of the method in terms of the cubic root of the number of degrees of freedom, which indeed resembles its counterpart for the source problem, see [34, Theorem 3].

Test case 4: checkerboard diffusivity tensor. As a final test, we consider as a physical domain the square $\Omega_4 = (-1,1)^2$, and we focus our attention to the checkerboard benchmark, that is, we fix in (3) $V = 0$ and we define the diffusivity tensor as follows:

$$\mathbb{K}(x,y) = \varrho(x,y)\mathbb{I} \quad \text{where} \quad \varrho(x,y) = \begin{cases} \varepsilon & \text{in } (-1,0)^2 \cup (0,1)^2 \\ 1 & \text{elsewhere.} \end{cases} \tag{39}$$

The eigenfunctions could be singular at the center of the checkerboard, that is, at the origin of the axes. Therefore, in addition to the h-version of the method, we also consider the hp-version with a distribution of the "polynomial" degrees as in (37) with $\mu = 1$, and geometrically graded meshes with grading parameter $\sigma = 0.5$, as those depicted in Figure 5.

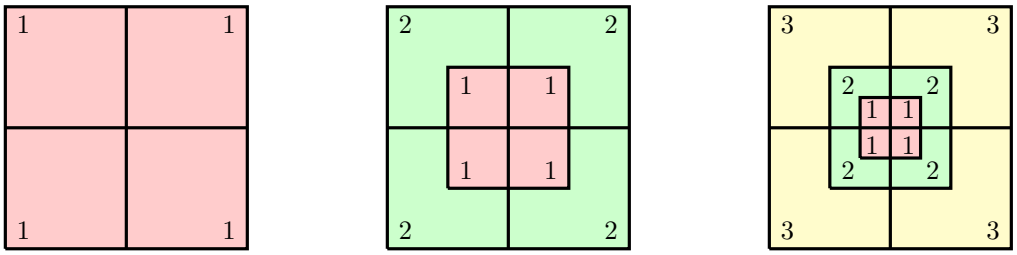

Fig. 5. First three meshes $\mathcal{T}_0$, $\mathcal{T}_1$, and $\mathcal{T}_2$, and the distribution of the "polynomial" degree for the approximation of eigenfunctions and eigenvalues of the checkerboard benchmark on the square domain Ω_4. The 0-th, the 1-st, and the 2-nd layers are highlighted in red, green, and yellow colors, respectively. The layers are constructed refining only towards the center of the checkerboard.

It is worthwhile to underline that the regularity of the solution to the associated source problem (6) decreases as $\varepsilon \to 0$ in (39). In [61, Figure 1], such a regularity was pinpointed for some specific choices of ε.

For this test case, we fix homogeneous Neumann boundary conditions. In order to test the method, we compare our discrete eigenvalues with those in [66]. In Figures 6 and 7, we show the performance of the h- and of the hp-versions on a sequence of uniform Cartesian meshes (conforming with respect to the discontinuities of the diffusivity tensor) and on the sequence of graded meshes in Figure 5, for two different "checkerboard" parameters ε in (39), respectively. More precisely, we study the convergence to the first four distinct eigenvalues, with parameters $\varepsilon = 2$ and 10^8.

Again, the exponential convergence of the hp-version of the method in terms of the cubic root of the degrees of freedom is in accordance with [34, Theorem], which is the analogous result for the source problem. We underline that the poor convergence rate for the second and third eigenvalues when $\varepsilon = 10^8$ is due to the poor accuracy of the exact eigenvalues computed in [66]. Importantly, the method is extremely robust for choices of both very high and moderate ε.

5. Conclusion

We analyzed the p-version of the virtual element method for elliptic problems with variable diffusivity tensor and reaction term. Particular emphasis was stressed on p-best interpolation estimates in enhanced virtual element spaces and on a careful investigation of the stabilization terms. Such analysis was instrumental to derive the a priori p-convergence estimate for the eigenvalue problems.

A wide set of numerical results, including experiments with the hp-version of the method, was presented in order to underline the superiority of the p- and hp-versions of the method over the h- one.

Acknowledgements. Lorenzo Mascotto has been funded by the Austrian Science Fund (FWF) through the project F 65. The work of Ondřej Čertík and Gianmarco Manzini was supported by the Laboratory Directed Research and Development Program (LDRD), U.S. Department of Energy Office of Science, Office of Fusion Energy Sciences, and the DOE Office of Science Advanced Scientific Computing Research (ASCR) Program in Applied Mathematics Research, under the auspices of the National Nuclear Security Administration of the U.S. Department of Energy by Los Alamos National Laboratory, operated by Los Alamos National Security LLC under contract DE-AC52-06NA25396.

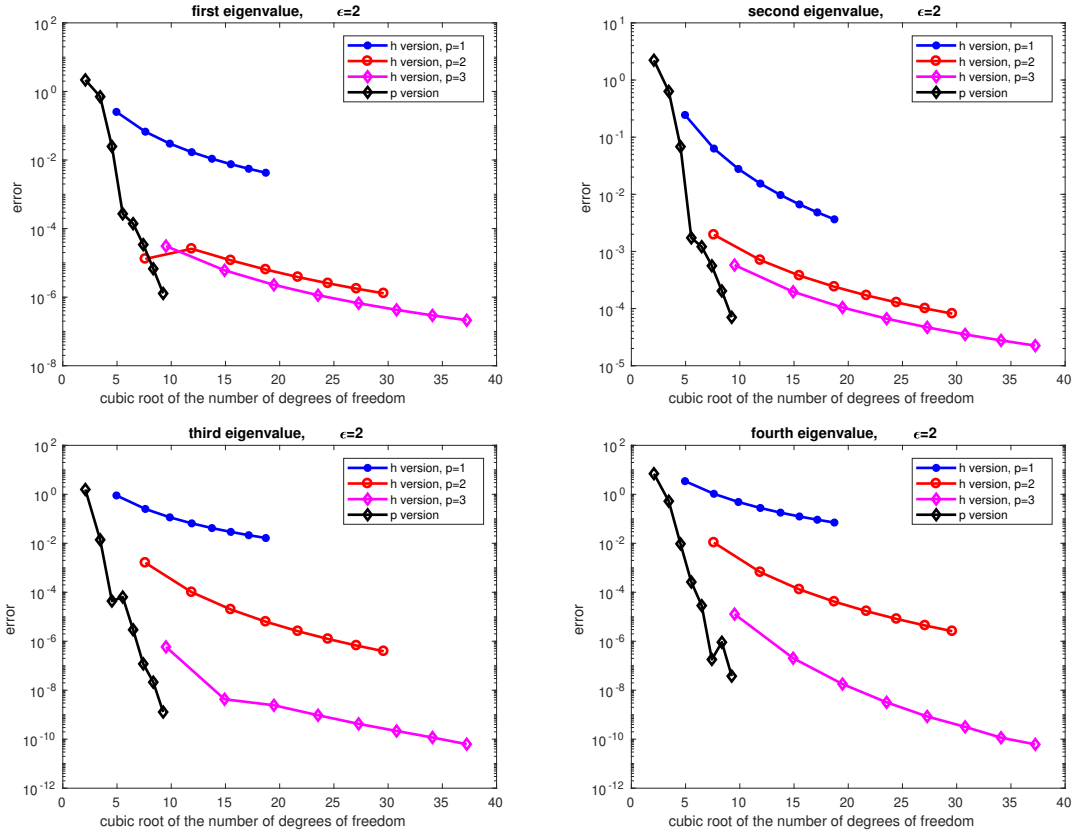

Fig. 6. Convergence of the error (35) for the first distinct Neumann four eigenvalues of the "checkerboard" operator with $\varepsilon = 2$ on the square domain Ω_4 employing the h-version with $p = 1$, 2, and 3 and the hp-version of the method. On the x-axis, we plot the cubic root of the number of degrees of freedom. The stabilizations $\widetilde{S}_1^K$ and S_0^K are defined in (36) and (29), respectively. The polynomial basis dual to the internal moments (11) is L^2 orthonormal elementwise. For the h-version we employ uniform Cartesian meshes, for the p-versions, we employ the meshes in Figure 3. The error curves plotted in the figure refer to the approximation of the problem eigenvalues as follows: *top-left panel:* first eigenvalue; *top-right panel:* second eigenvalue; *bottom-left panel:* third eigenvalue; *bottom-right panel:* fourth eigenvalue.

The authors are grateful to Dr. Joscha Gedicke from the University of Vienna for useful discussions regarding various aspects of the approximation of eigenvalues by means of Galerkin methods.

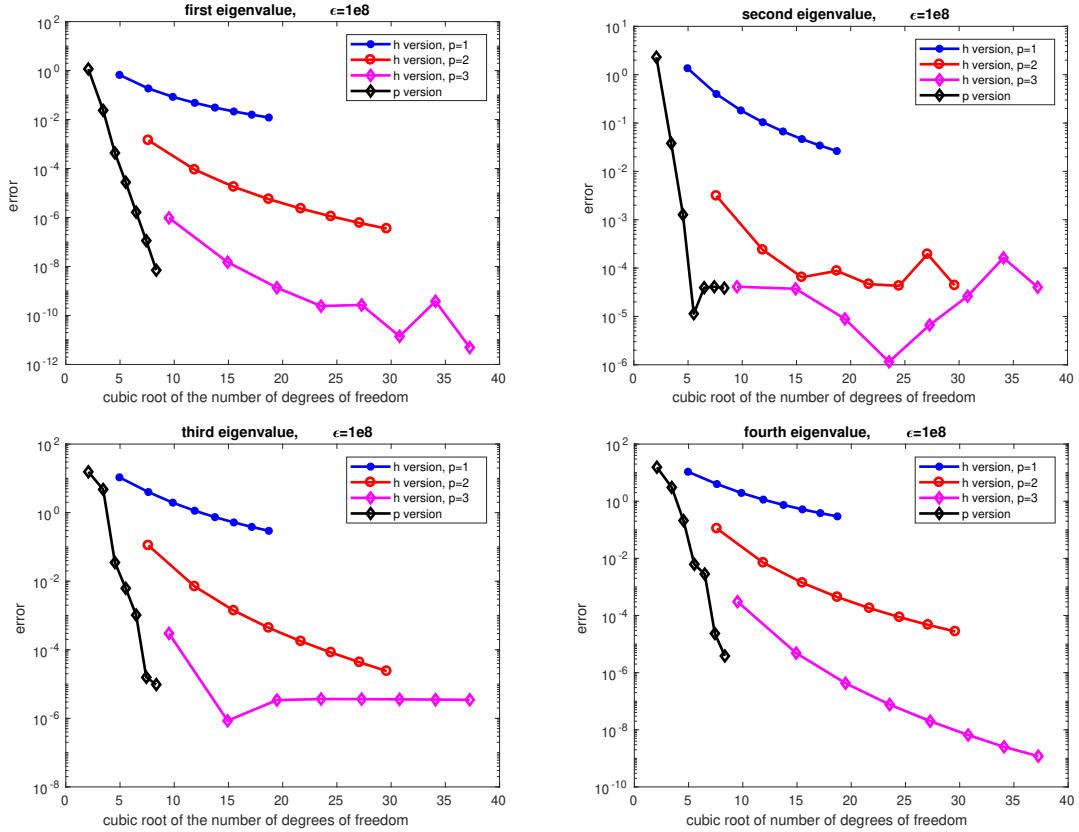

Fig. 7. Convergence of the error (35) for the first four distinct Neumann eigenvalues of the "checkerboard" operator with $\varepsilon = 10^8$ on the square domain Ω_4 employing the h-version with $p = 1$, 2, and 3 and the hp-version of the method. On the x-axis, we plot the cubic root of the number of degrees of freedom. The stabilizations $\widetilde{S}_1^K$ and S_0^K are defined in (36) and (29), respectively. The polynomial basis dual to the internal moments (11) is L^2 orthonormal elementwise. For the h-version we employ uniform Cartesian meshes, for the p-versions, we employ the meshes in Figure 3. The error curves plotted in the figure refer to the approximation of the problem eigenvalues as follows: *top-left panel:* first eigenvalue; *top-right panel:* second eigenvalue; *bottom-left panel:* third eigenvalue; *bottom-right panel:* fourth eigenvalue.

References

[1] B. Ahmad, A. Alsaedi, F. Brezzi, L.D. Marini, and A. Russo. Equivalent projectors for virtual element methods. *Comput. Math. Appl.*, 66(3):376–391, 2013.

[2] P. F. Antonietti, L. Beirão da Veiga, D. Mora, and M. Verani. A stream virtual element formulation of the stokes problem on polygonal meshes. *SIAM Journal on Numerical Analysis*, 52(1):386–404, 2014.

[3] P. F. Antonietti, L. Beirão da Veiga, S. Scacchi, and M. Verani. A C^1 virtual element method for the Cahn-Hilliard equation with polygonal meshes. *SIAM Journal on Numerical Analysis*, 54(1):34–56, 2016.

[4] P. F. Antonietti, N. Bigoni, and M. Verani. Mimetic discretizations of elliptic control problems. *Journal on Scientific Computing*, 56(1):14–27, 2013.

[5] P. F. Antonietti, F. Brezzi, and L. D. Marini. Bubble stabilization of Discontinuous Galerkin Methods. *Comput. Methods Appl. Mech. Engrg.*, 198(21-26):1651–1659, 2009.

[6] P. F. Antonietti, M. Bruggi, S. Scacchi, and M. Verani. On the Virtual Element Method for topology optimization on polygonal meshes: A numerical study. *Computers and Mathematics with Applications*, 74(5):1091–1109, 2017.

[7] P. F. Antonietti, A. Cangiani, J. Collis, Z. Dong, E. H. Georgoulis, S. Giani, and P. Houston. Review of Discontinuous Galerkin finite element methods for partial differential equations on complicated domains, 2016. G.R. Barrenechea et al. (eds.), Building Bridges: Connections and Challenges in Modern Approaches to Numerical Partial Differential Equations, *Lecture Notes in Computational Science and Engineering* 114:279–307.

[8] P. F. Antonietti, C. Facciolà, A. Russo, and M. Verani. Discontinuous Galerkin approximation of flows in fractured porous media on polygonal and polyhedral meshes, 2016. MOX Report 55/2016.

[9] P. F. Antonietti, L. Formaggia, A. Scotti, M. Verani, and N. Verzotti. Mimetic finite difference approximation of flows in fractured porous media. *M2AN Math. Model. Numer. Anal.*, 50(3):809–832, 2016.

[10] P. F. Antonietti, S. Giani, and P. Houston. *hp*–Version Composite Discontinuous Galerkin Methods for elliptic problems on complicated domains. *SIAM J. Sci. Comput.*, 35(3):A1417–A1439, 2013.

[11] P. F. Antonietti, G. Manzini, and M. Verani. The fully nonconforming Virtual Element method for biharmonic problems. *Mathematical Models & Methods in Applied Sciences*, 28(2), 2018.

[12] P. F. Antonietti, L. Mascotto, and M. Verani. A multigrid algorithm for the *p*-version of the virtual element method. *ESAIM Math. Model. Numer. Anal.*, 52(1):337–364, 2018.

[13] P. F. Antonietti and G. Pennesi. V–cycle multigrid algorithms for discontinuous Galerkin methods on non-nested polytopic meshes, 2017. MOX report 49/2017. Submitted.

[14] P. F. Antonietti, G. Pennesi, and Houston. Fast numerical integration on polytopic meshes with applications to discontinuous Galerkin finite element methods, 2018. MOX report 03/2018, Submitted.

[15] D. N. Arnold, F. Brezzi, B. Cockburn, and L. D. Marini. Unified analysis of discontinuous Galerkin methods for elliptic problems. *SIAM J. Numer. Anal.*, 39(5):1749–1779, 2001/2002.

[16] B. Ayuso de Dios, K. Lipnikov, and G. Manzini. The nonconforming virtual element method. *ESAIM: Mathematical Modelling and Numerical Analysis*, 50(3):879–904, 2016.

[17] I. Babuška and B. Guo. The *hp* version of the finite element method. *Comput. Mech.*, 1(1):21–41, 1986.

[18] I. Babuška and J. Osborn. *Eigenvalue problems*, volume *Handbook of Numerical Analysis, vol. II*, pages 641–787. Amsterdam: North-Holland, 1991.

[19] I. Babuška and M. Suri. The *hp* version of the finite element method with quasiuniform meshes. *ESAIM Math. Model. Numer. Anal.*, 21(2):199–238, 1987.

[20] R. F. W. Bader. A quantum theory of molecular structure and its applications. *Chem. Rev.*, 91(5):893–928, 1991.

[21] F. Bassi, L. Botti, and A. Colombo. Agglomeration-based physical frame DG discretizations: An attempt to be mesh free. *Math. Models Methods Appl. Sci.*, 24(8):1495–1539, 2014.

[22] L. Beirão da Veiga, F. Brezzi, A. Cangiani, G. Manzini, L. D. Marini, and A. Russo. Basic principles

of virtual element methods. *Mathematical Models & Methods in Applied Sciences*, 23:119–214, 2013.

[23] L. Beirão da Veiga, F. Brezzi, and L. D. Marini. Virtual elements for linear elasticity problems. *SIAM Journal on Numerical Analysis*, 51(2):794–812, 2013.

[24] L. Beirão da Veiga, F. Brezzi, L. D. Marini, and A. Russo. Mixed virtual element methods for general second order elliptic problems on polygonal meshes. *ESAIM: Mathematical Modelling and Numerical Analysis*, 50(3):727–747, 2016.

[25] L. Beirão da Veiga, K. Lipnikov, and G. Manzini. Arbitrary order nodal mimetic discretizations of elliptic problems on polygonal meshes. *SIAM Journal on Numerical Analysis*, 49(5):1737–1760, 2011.

[26] L. Beirão da Veiga, K. Lipnikov, and G. Manzini. *The Mimetic Finite Difference Method*, volume 11 of *MS&A. Modeling, Simulations and Applications*. Springer, I edition, 2014.

[27] L. Beirão da Veiga, C. Lovadina, and D. Mora. A virtual element method for elastic and inelastic problems on polytope meshes. *Computer Methods in Applied Mechanics and Engineering*, 295:327–346, 2015.

[28] L. Beirão da Veiga and G. Manzini. A virtual element method with arbitrary regularity. *IMA Journal on Numerical Analysis*, 34(2):782–799, 2014. DOI: 10.1093/imanum/drt018, (first published online 2013).

[29] L. Beirão da Veiga and G. Manzini. Residual a posteriori error estimation for the virtual element method for elliptic problems. *ESAIM: Mathematical Modelling and Numerical Analysis*, 49:577–599, 2015.

[30] L. Beirão da Veiga, G. Manzini, and M. Putti. Post-processing of solution and flux for the nodal mimetic finite difference method. *Numerical Methods for PDEs*, 31(1):336–363, 2015.

[31] L. Beirão da Veiga, F. Brezzi, A. Cangiani, G. Manzini, L.D. Marini, and A. Russo. Basic principles of virtual element methods. *Math. Models Methods Appl. Sci.*, 23(01):199–214, 2013.

[32] L. Beirão da Veiga, F. Brezzi, L. D. Marini, and A. Russo. Virtual element method for general second-order elliptic problems on polygonal meshes. *Math. Models Methods Appl. Sci.*, 26(4):729–750, 2016.

[33] L. Beirão da Veiga, A. Chernov, L. Mascotto, and A. Russo. Basic principles of *hp* virtual elements on quasiuniform meshes. *Math. Models Methods Appl. Sci.*, 26(8):1567–1598, 2016.

[34] L. Beirão da Veiga, A. Chernov, L. Mascotto, and A. Russo. Exponential convergence of the *hp* virtual element method with corner singularity. *Numer. Math.*, 138(3):581–613, 2018.

[35] L. Beirão da Veiga, F. Dassi, and A. Russo. High-order virtual element method on polyhedral meshes. *Comput. Math. Appl.*, 74(5):1110–1122, 2017.

[36] L. Beirão da Veiga, C. Lovadina, and A. Russo. Stability analysis for the virtual element method. *Math. Models Methods Appl. Sci.*, 27(13):2557–2594, 2017.

[37] L. Beirão da Veiga, G. Manzini, and L. Mascotto. A posteriori error estimation and adaptivity in *hp* virtual element. arXiv.org, 2018. *https://arxiv.org/abs/1804.07898*.

[38] L. Beirão da Veiga, D. Mora, G. Rivera, and R. Rodríguez. A virtual element method for the acoustic vibration problem. *Numer. Math.*, 136(3):725–763, 2017.

[39] M. F. Benedetto, S. Berrone, S. Pieraccini, and S. Scialò. The virtual element method for discrete fracture network simulations. *Computer Methods in Applied Mechanics and Engineering*, 280(0):135 – 156, 2014.

[40] S. Berrone, A. Borio, and G. Manzini. SUPG stabilization for the nonconforming virtual element method for advection-diffusion-reaction equations. *Computer Methods in Applied Mechanics and Engineering*, 340:500–529, 2018.

[41] D. Boffi. Finite element approximation of eigenvalue problems. *Acta Numer.*, 19:1–120, 2010.

[42] D. Boffi, F. Brezzi, and L. Gastaldi. On the problem of spurious eigenvalues in the approximation of linear elliptic problems in mixed form. *Math. Comp.*, 69(229):121–140, 2000.

[43] S. C. Brenner and L.-Y.. Sung. Virtual element methods on meshes with small edges or faces. *Math. Models Methods Appl. Sci.*, 268(07):1291–1336, 2018.

[44] F. Brezzi, A. Buffa, and K. Lipnikov. Mimetic finite differences for elliptic problems. *ESAIM: Mathematical Modelling and Numerical Analysis*, 43(2):277–295, 2009.

[45] F. Brezzi, R. S. Falk, and L. D. Marini. Basic principles of mixed virtual element methods. *ESAIM.*

Mathematical Modelling and Numerical Analysis, 48(4):1227–1240, 2014.

[46] F. Brezzi, K. Lipnikov, and M. Shashkov. Convergence of mimetic finite difference method for diffusion problems on polyhedral meshes with curved faces. *Math. Models Methods Appl. Sci.*, 16(2):275–297, 2006.

[47] F. Brezzi, G. Manzini, D. Marini, P. Pietra, and A. Russo. Discontinuous Galerkin approximations for elliptic problems. *Numerical Methods for Partial Differential Equations. An International Journal*, 16(4):365–378, 2000.

[48] F. Brezzi and L. D. Marini. Virtual element methods for plate bending problems. *Computer Methods in Applied Mechanics and Engineering*, 253:455–462, 2013.

[49] V. Calo, M. Cicuttin, Q. Deng, and A. Ern. Spectral approximation of elliptic operators by the hybrid high-order method. *arXiv preprint arXiv:1711.01135*, 2017.

[50] A. Cangiani, Z. Dong, E. H. Georgoulis, and P. Houston. *hp-Version Discontinuous Galerkin Methods on Polygonal and Polyhedral Meshes*. Springer International Publishing, 2017.

[51] A. Cangiani, Z. Dong, and E.H. Georgoulis. *hp*-version space-time discontinuous Galerkin methods for parabolic problems on prismatic meshes. *SIAM Journal on Scientific Computing*, 39(4):A1251–A1279, 2017.

[52] A. Cangiani, F. Gardini, and G. Manzini. Convergence of the mimetic finite difference method for eigenvalue problems in mixed form. *Comput. Methods Appl. Mech. Engrg.*, 200(9-12):1150–1160, 2011.

[53] A. Cangiani, E. Georgoulis, and P. Houston. *hp*-version discontinuous Galerkin Methods on polygonal and polyhedral meshes. *Math. Models Methods Appl. Sci.*, 24(10):2009–2041, 2014.

[54] A. Cangiani, E. H. Georgoulis, T. Pryer, and O. J. Sutton. A posteriori error estimates for the virtual element method. *Numerische Mathematik*, pages 1–37, 2017.

[55] A. Cangiani, V. Gyrya, and G. Manzini. The non-conforming virtual element method for the Stokes equations. *SIAM Journal on Numerical Analysis*, 54(6):3411–3435, 2016.

[56] A. Cangiani, V. Gyrya, G. Manzini, and O. Sutton. Chapter 14: Virtual element methods for elliptic problems on polygonal meshes. In K. Hormann and N. Sukumar, editors, *Generalized Barycentric Coordinates in Computer Graphics and Computational Mechanics*, pages 1–20. CRC Press, Taylor & Francis Group, 2017.

[57] A. Cangiani, G. Manzini, A. Russo, and N. Sukumar. Hourglass stabilization of the virtual element method. *International Journal on Numerical Methods in Engineering*, 102(3-4):404–436, 2015.

[58] A. Cangiani, G. Manzini, and O. Sutton. Conforming and nonconforming virtual element methods for elliptic problems. *IMA Journal on Numerical Analysis*, 37:1317–1354, 2017. (online August 2016).

[59] S. Cao and L. Chen. Anisotropic error estimates of the linear virtual element method on polygonal meshes. *SIAM J. Numer. Anal.*, 56(5):2913–2939, 2018.

[60] O. Certík, F. Gardini, G. Manzini, and G. Vacca. The virtual element method for eigenvalue problems with potential terms on polytopic meshes. *Appl. Math.*, 63(3):333–365, 2018.

[61] P. Ciarlet Jr, E. Jamelot, and F. D. Kpadonou. Domain decomposition methods for the diffusion equation with low-regularity solution. *Comput. Math. Appl.*, 74(10):2369–2384, 2017.

[62] B. Cockburn, D. A. Di Pietro, and A. Ern. Bridging the Hybrid High-order and Hybridizable Discontinuous Galerkin Methods. *ESAIM Math. Model. Numer. Anal.*, 50(3):635–650, 2016.

[63] B. Cockburn, B. Dong, and J. Guzmán. A superconvergent LDG-Hybridizable Galerkin Method for second-order elliptic problems. *Math. Comp.*, 77(264):1887–1916, 2008.

[64] B. Cockburn, J. Gopalakrishnan, and R. Lazarov. Unified hybridization of discontinuous Galerkin, mixed, and continuous Galerkin methods for second order elliptic problems,. *SIAM Journal on Numerical Analysis*, 47(2):1319–1365, 2009.

[65] F. Dassi and L. Mascotto. Exploring high-order three dimensional virtual elements: bases and stabilizations. *Comput. Math. Appl.*, 75(9):3379–3401, 2018.

[66] M. Dauge. Benchmark computations for Maxwell equations for the approximation of highly singular solutions. Available at *https://perso.univ-rennes1.fr/monique.dauge/benchmax.html*.

[67] D. Davydov, T. Gerasimov, J.-P. Pelteret, and P. Steinmann. Convergence study of the *h*-adaptive PUM and the *hp*-adaptive FEM applied to eigenvalue problems in quantum mechanics. *Advanced Modeling and Simulation in Engineering Sciences*, 4(1):7, 2017.

[68] D. A. Di Pietro, J. Droniou, and G. Manzini. Discontinuous skeletal gradient discretisation methods on polytopal meshes. *Journal of Computational Physics*, 355:397–425, 2018.

[69] D. A. Di Pietro and A. Ern. *Mathematical aspects of discontinuous Galerkin methods*. Springer Science & Business Media, 2011.

[70] D. A. Di Pietro, A. Ern, and S. Lemaire. An arbitrary-order and compact-stencil discretization of diffusion on general meshes based on local reconstruction operators. *Comput. Methods Appl. Math.*, 14(4):461–472, 2014.

[71] J. Droniou. Finite volume schemes for diffusion equations: Introduction to and review of modern methods. *Mathematical Models and Methods in Applied Sciences*, 24(08):1575–1619, 2014.

[72] J. Droniou, R. Eymard, T. Gallouet, and R. Herbin. Gradient schemes: a generic framework for the discretisation of linear, nonlinear and nonlocal elliptic and parabolic equations. *Math. Models Methods Appl. Sci.*, 23(13):2395–2432, 2013.

[73] R. Eymard, C. Guichard, and R. Herbin. Small-stencil 3D schemes for diffusive flows in porous media. *ESAIM Math. Model. Numer. Anal.*, 46(2):265–290, 2012.

[74] M. Frittelli and I. Sgura. Virtual element method for the Laplace Beltrami equation on surfaces, 2018 (accepted). arXiv:1612.02369v1.

[75] A. L. Gain, C. Talischi, and G. H. Paulino. On the virtual element method for three-dimensional linear elasticity problems on arbitrary polyhedral meshes. *Computer Methods in Applied Mechanics and Engineering*, 282:132–160, 2014.

[76] F. Gardini, G. Manzini, and G. Vacca. The nonconforming virtual element method for eigenvalue problems. *http://arxiv.org/abs/1802.02942*, 2018.

[77] F. Gardini and G. Vacca. Virtual element method for second-order elliptic eigenvalue problems. *IMA J. Numer. Anal.*, 38(4):2026–2054, 2018.

[78] S. Giani. *hp*-adaptive composite discontinuous Galerkin methods for elliptic eigenvalue problems on complicated domains. *Appl. Math. Comput.*, 267:604–617, 2015.

[79] S. Giani, L. Grubišić, and J. S. Ovall. Error control for *hp*-adaptive approximations of semi-definite eigenvalue problems. *Computing*, 95(1):235–257, 2013.

[80] S. Giani and P. Houston. *hp*–adaptive composite discontinuous Galerkin methods for elliptic problems on complicated domains. *Numer. Methods Partial Differential Equations*, 30(4):1342–1367, 2014.

[81] D. J. Griffiths. *Introduction to Quantum Mechanics*. Prentice Hall Inc, Upper Saddle, New Jersey, USA, 1995.

[82] E. K. U. Gross and R. M. Dreizler. *Density functional theory*, volume 337. Springer Science & Business Media, 2013.

[83] V. Gyrya, K. Lipnikov, and G. Manzini. The arbitrary order mixed mimetic finite difference method for the diffusion equation. *ESAIM: Mathematical Modelling and Numerical Analysis*, 50(3):851–877, 2016.

[84] W. K. Heisenberg. Uber quantumtheoretische Umdeutung kinematischer und mechanischer Beziehungen,. *Z. Phys*, 33, 1925. English translation in B. L. van der Waerden, Sources of quantum mechanics, North Holland Amsterdam 1967.

[85] J. Hyman, M. Shashkov, and S. Steinberg. The numerical solution of diffusion problems in strongly heterogeneous non-isotropic materials. *J. Comput. Phys.*, 132(1):130–148, 1997.

[86] K. Lipnikov and G. Manzini. A high-order mimetic method on unstructured polyhedral meshes for the diffusion equation. *Journal of Computational Physics*, 272:360–385, 2014.

[87] K. Lipnikov, G. Manzini, J. D. Moulton, and M. Shashkov. The mimetic finite difference method for elliptic and parabolic problems with a staggered discretization of diffusion coefficient. *Journal of Computational Physics*, 305:111 – 126, 2016.

[88] K. Lipnikov, G. Manzini, and M. Shashkov. Mimetic finite difference method. *Journal of Computational Physics*, 257 – Part B:1163–1227, 2014. Review paper.

[89] G. Manzini, K. Lipnikov, J. D. Moulton, and M. Shashkov. Convergence analysis of the mimetic finite difference method for elliptic problems with staggered discretizations of diffusion coefficients. *SIAM Journal on Numerical Analysis*, 55(6):2956–2981, 2017.

[90] G. Manzini, A. Russo, and N. Sukumar. New perspectives on polygonal and polyhedral finite element

methods. *Mathematical Models & Methods in Applied Sciences*, 24(8):1621–1663, 2014.

[91] L. Mascotto. Ill-conditioning in the virtual element method: stabilizations and bases. *Numer. Methods Partial Differential Equations*, 34(4):1258–1281, 2018.

[92] D. Mora, G. Rivera, and R. Rodríguez. A virtual element method for the Steklov eigenvalue problem. *Math. Models Methods Appl. Sci.*, 25(08):1421–1445, 2015.

[93] D. Mora, G. Rivera, and R. Rodriguez. A posteriori error estimates for a virtual elements method for the Steklov eigenvalue problem. *Comput. Math. Appl.*, 74(9):2172–2190, 2017.

[94] D. Mora, G. Rivera, and I. Velásquez. A virtual element method for the vibration problem of Kirchhoff plates. *ESAIM Math. Model. Numer. Anal.*, 52(4):1437–1456, 2018.

[95] D. Mora and I. Velásquez. A virtual element method for the transmission eigenvalue problem. *Math. Models Methods Appl. Sci.*, 2018. doi: *https://doi.org/10.1142/S0218202518500616*.

[96] A. Okabe, B. Boots, K. Sugihara, and S.N. Chiu. *Spatial Tesselations: Concepts and Applications of Voronoi Diagrams*. John Wiley & sons, England, second edition, 1988.

[97] S. Rjasanow and S. Weißer. Higher order BEM-based FEM on polygonal meshes. *SIAM J. Numer. Anal.*, 50(5):2357–2378, 2012.

[98] S. Sauter. *hp*-finite elements for elliptic eigenvalue problems: error estimates which are explicit with respect to λ, h, and p. *SIAM J. Numer. Anal.*, 48(1):95–108, 2010.

[99] C. Schwab. *p- and hp- Finite Element Methods: Theory and Applications in Solid and Fluid Mechanics*. Clarendon Press Oxford, 1998.

[100] N. Sukumar and A. Tabarraei. Conforming Polygonal Finite Elements. *Internat. J. Numer. Methods Engrg.*, 61(12):2045–2066, 2004.

[101] A. Tabarraei and N. Sukumar. Extended Finite Element Method on polygonal and quadtree meshes. *Comput. Methods Appl. Mech. Engrg.*, 197(5):425–438, 2008.

[102] G. Vacca. An H^1-conforming virtual element for Darcy and Brinkman equations. *Mathematical Models & Methods in Applied Sciences*, 28(1):159–194, 2018.

[103] W. Yang and P. W. Ayers. Density-functional theory. In *Computational Medicinal Chemistry for Drug Discovery*, pages 103–132. CRC Press, 2003.

[104] J. Zhao, S. Chen, and B. Zhang. The nonconforming virtual element method for plate bending problems. *Mathematical Models & Methods in Applied Sciences*, 26(9):1671–1687, 2016.